

**Title:** Islet-derived eATP fuels autoreactive CD8<sup>+</sup> cells and facilitates the onset of type 1 diabetes

**Short running title:** eATP/P2X7R axis in T1D

**Authors:** Sara Tezza<sup>1#</sup>, Moufida Ben Nasr<sup>1,2#</sup>, Francesca D'Addio<sup>1,2</sup>, Andrea Vergani<sup>1</sup>, Vera Usuelli<sup>2</sup>, Simonetta Falzoni<sup>3</sup>, Roberto Bassi<sup>1</sup>, Sergio Dellepiane<sup>1</sup>, Carmen Fotino<sup>4</sup>, Chiara Rossi<sup>5</sup>, Anna Maestroni<sup>2</sup>, Anna Solini<sup>6</sup>, Domenico Corradi<sup>7</sup>, Elisa Giani<sup>8</sup>, Chiara Mameli<sup>8</sup>, Federico Bertuzzi<sup>9</sup>, Marcus Guy Pezolesi<sup>10</sup>, Clive H. Wasserfall<sup>11</sup>, Mark A. Atkinson<sup>11</sup>, Ernst-Martin Füchtbauer<sup>12</sup>, Camillo Ricordi<sup>4</sup>, Franco Folli<sup>13,14</sup>, Francesco Di Virgilio<sup>3</sup>, Antonello Pileggi<sup>4</sup>, Sirano Dhe-Paganon<sup>15</sup>, Gian Vincenzo Zuccotti<sup>2,8</sup> and Paolo Fiorina<sup>1,2,16\*</sup>

**Affiliations:** <sup>1</sup>Nephrology Division, Boston Children's Hospital, Harvard Medical School, Boston, USA; <sup>2</sup>International Center for T1D, Pediatric Clinical Research Center Fondazione Romeo ed Enrica Invernizzi, Department of Biomedical and Clinical Science L. Sacco, University of Milan, Italy; <sup>3</sup>Department of Morphology, Surgery and Experimental Medicine, University of Ferrara, Italy; <sup>4</sup>Diabetes Research Institute, University of Miami, USA; <sup>5</sup>Department of Clinical and Experimental Medicine and <sup>6</sup>Department of Surgical, Medical and Critical Area Pathology, University of Pisa, Italy; <sup>7</sup>Pathology and Laboratory Medicine, University of Parma, Italy; <sup>8</sup>Pediatric Clinical Research Center Fondazione Romeo ed Enrica Invernizzi, Department of Biomedical and Clinical Science L. Sacco, University of Milan, Department of Pediatrics-Children Hospital Buzzi, Milan, Italy; <sup>9</sup>Diabetology Unit, ASST Grande Ospedale Metropolitano Niguarda, Milan, Italy; <sup>10</sup>Division of Nephrology and Hypertension, Diabetes and Metabolism Center, University of Utah, Salt Lake City, UT; <sup>11</sup>Department of Pathology, Immunology and Laboratory Medicine, University of Florida, Gainesville, FL; <sup>12</sup>Department of Molecular Biology and Genetics, Aarhus, Denmark; <sup>13</sup>Department of Medicine, University of Texas, Health System, San Antonio, TX; <sup>14</sup>ASST Santi Paolo e Carlo, Milan, Italy; <sup>15</sup>Structural Biology Center, Dana-Farber Cancer Institute, Boston, MA; <sup>16</sup> Division of Endocrinology, ASST Sacco Fatebenefratelli-Sacco, Milan, Italy; #These authors contributed equally to this work; \*Corresponding author.

**Abstract word count:** 160

**Total Word count:** 5,527

**Figures:** 6

**Tables:** 1

**Keywords:** Type 1 diabetes, ATP, P2X7R, CD8 T cells

**\*Corresponding Author:**

Paolo Fiorina, MD PhD

Nephrology Division

Boston Children's Hospital, Harvard Medical School

Enders Building 5<sup>th</sup> floor, Room EN511

300 Longwood Ave Boston, MA 02115

Tel: 617-919-2624

ORCID: 0000-0002-1093-7724

**E-mail:** [paolo.fiorina@childrens.harvard.edu](mailto:paolo.fiorina@childrens.harvard.edu)

**Abstract**

Extracellular ATP (eATP) activates T cells by engaging the P2X7R receptor. We identified two loss-of-function P2X7R mutations that are protective against type 1 diabetes (T1D) and thus hypothesized that eATP/P2X7R signaling may represent an early step in T1D onset. Specifically, we observed that in newly diagnosed T1D patients, P2X7R is upregulated on CD8<sup>+</sup> effector T cells in comparison to healthy controls. eATP is released at high levels by human/murine islets *in vitro* in high-glucose/inflammatory conditions, thus upregulating P2X7R on CD8<sup>+</sup> T cells *in vitro*. P2X7R blockade with oxidized ATP (oATP) reduces the CD8<sup>+</sup> T cell-mediated autoimmune response *in vitro* and delays diabetes onset in NOD mice. Autoreactive CD8<sup>+</sup> T cell activation is highly dependent upon eATP/P2X7R-mediated priming, while a novel sP2X7R recombinant protein abrogates changes in metabolism and the autoimmune response associated with CD8<sup>+</sup> T cells. eATP/P2X7R signaling facilitates the onset of autoimmune T1D by fueling autoreactive CD8<sup>+</sup> cells and therefore represents a novel targeted therapeutic for the disorder.

## Introduction

Understanding of the immunological mechanisms underlying type 1 diabetes (T1D) development has broadened dramatically<sup>1,2</sup>, which has aided in design of potential immunoregulatory treatments capable of preventing and/or curing the disease<sup>3,4</sup>. A key goal of these approaches is to revert hyperglycemia in T1D patients or to prevent the onset of disease in individuals at high-risk<sup>5</sup>. However, despite much effort, an immune-based cure for T1D does not exist, and concern remains due to the increased risk of mortality associated with the disorder<sup>6</sup>. Reversal of diabetes can currently be obtained only with pancreatic islet<sup>7,8</sup> or whole pancreas transplantation, which confers a different set of complications and sub-optimal long-term outcomes<sup>9</sup>.

The purine adenosine 5'-triphosphate (ATP) is a small molecule<sup>10</sup> present in high concentrations within cells that can be released into the extracellular compartment as extracellular ATP (eATP) by damaged or necrotic cells<sup>11</sup> and by activated immune cells<sup>12,13</sup>. Once in the extracellular space, eATP can be sensed by ionotropic purinergic P2X receptors (7 receptors named P2X1-P2X7 receptors, or P2XRs)<sup>14-16</sup> as a fundamental step in immune cell activation<sup>17-20</sup>. In particular, P2X7R<sup>12,16,21,22</sup> has been linked to T cell activation, serving as a signal amplification mechanism for antigen recognition<sup>17</sup>, Th1/Th17 generation<sup>1,23</sup> and allograft rejection<sup>24</sup>. Interestingly, ATP is co-secreted with insulin by pancreatic  $\beta$  cells<sup>25,26</sup>. We hypothesize that eATP-driven/P2X7R-mediated immunity may be activated by pancreatic  $\beta$ -cell injury (e.g. viruses, stresses), when  $\beta$  cells release eATP and prime passenger leukocytes<sup>25,26</sup>. During the autoimmune response, eATP can also be released by cytotoxic T cells, thus creating a feedback loop that sustains the autoimmune response and inflammation<sup>1,23,24</sup>. Understanding the potential role of the purinergic system in the priming of the T cell-mediated anti-islet immune response in the pathogenesis of T1D will contribute to design of potential therapies for T1D, especially considering P2X7R inhibitors are available for human use<sup>27,28</sup>.

## **Research Design and Methods**

### ***Genetic studies***

A detailed description of the Joslin Study of Genetics of Kidneys in Diabetes (GoKinD) was recently published<sup>1</sup>. Unrelated European-American individuals from the GoKinD (n=3410) and the Exome Sequencing Project (ESP6500, n=8600) cohort database were interrogated for P2X7R genetic variants. The FREQ Procedure of the SAS system was used to determine the frequency of each single nucleotide polymorphism (SNP) of human P2X7R. Odds ratios for each SNP were calculated, and Bonferroni correction was applied to each P value.

### ***Patients***

Blood samples were obtained from new onset diabetic patients, long-term diabetic patients, T2D patients and from healthy controls, who were enrolled under an Institutional Review Board committee approval (Table 1). Peripheral blood mononuclear cell (PBMC) fractions were isolated from 20 ml whole blood by Ficoll density gradient centrifugation.

### ***Human antibodies***

The following antibodies were used for flow cytometric analysis: phycoerythrin (PE)-Cy7-conjugated anti-human CCR7, allophycocyanin (APC)-labeled anti-human CD45RO, Alexa Fluor 700-conjugated CD4, V500-conjugated anti-human CD8, APC-labeled anti-human CD11c, and PE-Cy7-conjugated anti-human CD19 were purchased from BD Biosciences (San Jose, CA), eBioscience (San Diego, CA) or Life Technologies (Carlsbad, CA). Fluorescein isothiocyanate (FITC)-conjugated anti-human P2X7R was purchased from Alomone Labs (Jerusalem, Israel).

### ***Human flow cytometric analysis***

To characterize P2X7R expression on T cells, human PBMCs isolated from healthy controls, new onset T1D patients, long-standing T1D patients and T2D patients were stained with anti-human CD4, CD8, CD11c or CD19 and anti-human P2X7R. Human P2X7R expression on CD4<sup>+</sup> and CD8<sup>+</sup> effector and

central memory T cells was determined by staining for P2X7R, CD45RO, CCR7 and CD4 or CD8, respectively. The number of cells was calculated by acquiring  $10^5$  events in the lymphocyte gate (SSC-FSC) by flow cytometric analysis.

### ***Intracellular staining for flow cytometry***

Anti-human CD4, CD8, CD25, interferon- $\gamma$  (IFN- $\gamma$ ) and interleukin-17 (IL-17) were purchased from BD Biosciences, Becton-Dickinson (Franklin Lakes, NJ), or Life Technologies, and anti-mouse FITC-labeled P2X7R was purchased from Alomone Labs. Resting cells were activated with PMA (5 ng/ml), ionomycin (500 ng/ml) and brefeldin A (2  $\mu$ M; Sigma-Aldrich, St. Louis, MO) for 3 h. Cells were harvested in FACS tubes and placed on ice. Cells were then washed with FACSFlow (BD Biosciences) and processed for intracellular cytokine staining with 0.5% saponin (Sigma-Aldrich) and 2% formaldehyde for fixation and permeabilization. Antibodies used for intracellular staining (BD Biosciences unless stated otherwise) were PE-conjugated anti-IL-17, and allophycocyanin-conjugated anti-IFN- $\gamma$ .

### ***Human ELISpot assay***

An ELISpot assay was used to measure the number of IFN- $\gamma$ -producing cells according to the manufacturer's protocol (BD Biosciences) as previously shown by our group<sup>2</sup>.  $2 \times 10^6$  PBMCs, isolated from T1D patients, were cultured for 48h in the presence of IA-2 (100  $\mu$ g/ml) peptide. At day 1 after stimulation, 500  $\mu$ l media was added to the culture. Cells were collected at day 2 and plated in a human IFN- $\gamma$  ELISpot assay with or without oATP or CE-224,535 at different concentrations (1, 10 or 100  $\mu$ M). Spots were counted using an A.El.VIS ELISpot Reader (A.El.VIS GmbH, Hannover, Germany).

In another assay, we isolated CD8<sup>+</sup> T cells using microbeads from PBMCs obtained from healthy subjects, and  $5 \times 10^5$  CD8<sup>+</sup> T cells were incubated with a mixture of vaccine antigens (Diftavax) (tetanus toxoid, difteria, and hemophilus) for 24 hours with/without adding the receptor antagonists oxidized

ATP (oATP) or CE-224,535. Using an ELISpot assay, we tested the ability of both P2X7R receptor antagonists (oATP or CE-224,535) to halt the activation of CD8<sup>+</sup> T cells when exposed to vaccination antigens.

### ***Extracellular ATP measurements***

Supernatants were collected from a beta cell line (Beta-lox5, kindly provided by Prof. Clayton Mathews, University of Florida), previously cultured and exposed to IFN- $\gamma$  (2 ng/ml, R&D Systems [Minneapolis, MN] +/- IL-1 $\beta$  (1,000 U/ml, Peprotech [Rocky Hill, NJ]) for 3 days to replicate pro-inflammatory/diabetogenic conditions as previously described<sup>3,4</sup> under high-glucose conditions (35 mM) for eATP quantification. We further compared eATP levels measured in supernatants of beta cells with that of other cell lines (Caco-2) and of PBMCs isolated from T1D subjects (2x10<sup>6</sup> cells/well), cultured in the same conditions. Finally, we also collected supernatants from PBMCs of T1D subjects previously exposed to IA-2 or Pediacel (Sanofi Pasteur), Diftavax or anti-CD3/CD28 (as described above) to quantify eATP. Briefly, supernatant samples were resuspended in ATP assay buffer (300–400 ml) on ice and spun at 14,000 g for 5 min at 4°C, after which the supernatant was transferred to a 10 kDa molecular weight cutoff spin filter and spun at 14,000 g for 5 min at 4°C to be deproteinized. The samples were transferred to a 96-well plate and the fluorescence (lex = 535 nm, lem = 587 nm) was measured using a SpectraMax Paradigm Multi-Mode Detection Platform (Molecular Devices, Sunnyvale, CA). The background was subtracted from the measurement, and the amount of ATP present in the samples was determined from the standard curve. Results obtained were normalized to the number of cells.

### ***Mice***

Female BALB/c, NOD/ShiLtJ (NOD) at 4 and 8 weeks of age, female NOD/SCID, BDC2.5 TCR NOD (NOD-BDC2.5), NOD.Tcr NY8.3 (8.3-NOD) and NOD-P2X7R knock out at 8 weeks of age were obtained from the Jackson Laboratory (Bar Harbor, Maine). Female pmeLUC transgenic mice were kindly provided by collaboration with the Danish Center for Genetically Modified Mice represented by

Ernst-Martin Fuchtbauer, Department of Molecular Biology Aarhus University. Transgenic mice were generated by injection of the pmeLUC DNA construct into B6D2F1/J mouse pronuclei. All mice were cared for and used in accordance with institutional guidelines approved by the Harvard Medical School Institutional Animal Care and Use Committee.

## Results

### ***P2X7R loss-of-function mutation protects against T1D***

We first analyzed unrelated European-American patients from the Genetics of Kidneys in Diabetes (GoKinD, n=1705) and the Exome Sequencing Project (ESP6500, n=4300) cohorts, in order to identify any associations between P2X7R genetic variants and the T1D condition. The human *P2X7R* gene is a highly polymorphic gene that spans 52 kb and maps to the chromosomal region 12q24.31. Interrogation of the GoKinD and ESP6500 databases revealed 8 single nucleotide polymorphisms (SNPs) in the human *P2X7R* gene (Fig. 1A). Among these SNPs, the rs3751143 and rs7958311 point mutations are non-synonymous SNPs (nsSNPs) with an alanine substitution for glutamate at amino acid position 496 (1513A>C, E496A) and an arginine substitution for histidine at position 270 (835G>A, R270H) respectively, leading to P2X7R loss-of-function. Both rs3751143 and rs7958311 appeared to be protective against the development of T1D (rs3751143: odds ratio [OR]=0.8, p=0.0006; rs7958311: OR=0.86, p=0.01, respectively) (Fig. 1A-B), even after a conservative Bonferroni correction.

### ***Elevated P2X7R<sup>+</sup> T cells are evident in newly diagnosed T1D patients and P2X7R inhibitors reduce the human autoimmune response in vitro***

In order to understand the role of eATP/P2X7R signaling in T1D, we first analyzed eATP production during an autoimmune response *in vitro*. When PBMCs obtained from new onset T1D patients were challenged with the islet peptide IA-2, increased levels of eATP were evident in the supernatants (Fig. 1C). We then determined the P2X7R expression profile of different lymphocyte subpopulations in PBMCs obtained from patients with newly diagnosed and long-standing T1D as well as healthy controls

and T2D patients (Fig. 1D-S; Supplementary Fig. S1A). A higher number of P2X7R<sup>+</sup>CD4<sup>+</sup> (Fig. 1D-E), P2X7R<sup>+</sup>CD4<sup>+</sup>CD45RO<sup>+</sup>CCR7<sup>+</sup> effector memory T cells (Fig. 1F-G), P2X7R<sup>+</sup>CD8<sup>+</sup> (Fig. 1L-M) were evident in long-standing T1D patients as compared to healthy controls, T2D patients and newly diagnosed T1D patients. Increased numbers of P2X7R<sup>+</sup>CD4<sup>+</sup>CD45RO<sup>+</sup>CCR7<sup>-</sup> central memory T cells (although not statistically significant) (Fig. 1H-I), of P2X7R<sup>+</sup>CD8<sup>+</sup>CD45RO<sup>+</sup>CCR7<sup>+</sup> effector memory (Fig. 1N-O) and P2X7R<sup>+</sup>CD8<sup>+</sup>CD45RO<sup>+</sup>CCR7<sup>-</sup> central memory T cells (Fig. 1P-Q) were observed in newly diagnosed T1D patients as compared to healthy controls, T2D patients and long-standing T1D patients. While there was no difference in the numbers of P2X7R<sup>+</sup>CD19<sup>+</sup> cells (Fig. 1J-K) between groups, increased numbers of P2X7R<sup>+</sup>CD11c<sup>+</sup> cells (although not statistically significant) (Fig. 1R-S) were observed in newly diagnosed and long-standing T1D patients as compared to healthy controls and T2D patients. We further observed reduced expression of P2X7R<sup>+</sup>CD4<sup>+</sup>CD45RO<sup>+</sup>CCR7<sup>-</sup> central memory T cells (although not statistically significant) (Fig. 1H-I) and a significant reduction in the expression of P2X7R<sup>+</sup>CD8<sup>+</sup>CD45RO<sup>+</sup>CCR7<sup>+</sup> effector memory T cells (Fig. 1N-O) in T2D patients as compared to all other groups. To evaluate the benefit of targeting the eATP/P2X7R axis during the autoimmune response, two P2X7R inhibitors, oxidized ATP (oATP) and CE-224,535, were used in human autoimmune assays *in vitro*. In a 24-hour ELISpot assay, the T cell response against the islet peptide IA-2, measured as number of IFN- $\gamma$ -producing cells, was reduced by the addition of the P2X7R inhibitors oATP and CE-224,535 (Fig. 1T).

***Human CD8<sup>+</sup> cell function appears highly linked to eATP/P2X7R-signaling during the autoimmune response***

To further delineate the role of eATP/P2X7R signaling in CD4<sup>+</sup> and CD8<sup>+</sup> naïve T cells, we cultured CD4<sup>+</sup>CD25<sup>-</sup> and CD8<sup>+</sup> T cells in the presence of IA-2 and measured the percentage of IFN- $\gamma$ <sup>+</sup> and IL-17<sup>+</sup> cells generated during an autoimmune response by flow cytometry. The CD4 T cell-associated autoimmune response appeared to be primarily mediated by IFN- $\gamma$ <sup>+</sup> cells, with few IL-17<sup>+</sup> cells being

generated (Fig. 1U-V); in fact, in both cases cytokines appeared to be predominantly produced by the  $CD4^+CD25^-P2X7R^-$  subpopulation and thus appeared independent of eATP/P2X7R signaling (Fig. 1U-V). In contrast, the  $CD8^+$  cell autoimmune response was mostly associated with IL-17 production, principally from the  $P2X7R^+CD8^+$  subpopulation, and therefore was strictly dependent upon eATP/P2X7R signaling (Fig. 1W-X).

***eATP is highly released by human/murine pancreatic islets in vitro during high-glucose/inflammatory conditions***

We then explored the ability of pancreatic islets to release eATP in response to various stimuli. First, pancreatic eATP release was evaluated *in vitro* during challenge with high glucose and with pro-inflammatory cytokines. Pancreata were harvested from pmLUC transgenic mice, which express luciferase on their cell membrane, and were cultured in the presence of different glucose concentrations. Luminescence was monitored at different time points during high-glucose challenge using an IVIS-Caliper luminometer (Fig. 2A). In this assay, the levels of bioluminescence observed are proportional to eATP concentration<sup>29</sup>. An increase in the extent of luminescence dependent on glucose level was evident (Fig. 2A-B, Supplementary Fig. S1B). We then purified islets from 10-week-old NOD/SCID mice and from deceased human donors and cultured them with either (i) normal glucose (control), (ii) a cocktail of cytokines composed of IL-1 $\beta$ , TNF- $\alpha$  and IFN- $\gamma$  (known to be involved in islet damage) or (iii) high glucose (HG, 25mM) (Fig. 2C-D). Both the cytokine cocktail and high-glucose conditions increased the release of eATP by murine and human pancreatic islets; indeed, the highest eATP release was observed following exposure to high glucose (Fig. 2C-D). We next challenged a human  $\beta$  cell line (Beta-lox5) in the presence of different stimuli (i.e. high glucose, IFN- $\gamma$  or IL-1 $\beta$ ) and quantified eATP release (Supplementary Fig. S1C). The same experiment was performed on a human intestinal Caco-2 cell line and on human PBMCs from T1D using all the aforementioned conditions including Diftavax and anti-

CD3/anti-CD28 stimulation (Supplementary Fig. S1D-E). Beta-lox5 cells released high levels of eATP, measured in the culture supernatant, as compared to other cell lines (Supplementary Fig. S1C-E).

***eATP is released by pancreatic islets in vivo during the early phase of diabetes onset in NOD mice***

To assess the *in vivo* release of eATP from pancreatic islets during the onset of autoimmune diabetes in NOD mice, HEK293-pmeLUC transgenic cells and D-luciferin were injected into the peritoneal cavity of NOD and BALB/c mice. HEK293-pmeLUC transgenic cells function as reporters of eATP concentration *in vivo*<sup>16</sup>. Please see Research Design and Methods for a description of the system. A stable luminescence signal was observed in BALB/c mice at different ages (Fig. 2E-F), while in NOD mice, the luminescence signal appeared higher than that which was obtained in BALB/c mice (Fig. 2E-F). A gradual disappearance of bioluminescence was evident over time in NOD mice, paralleling insulinitis progression and the autoimmune-mediated destruction of pancreatic islets (Fig. 2E-F). The area under the curve (AUC) of bioluminescence confirmed the increased eATP release in NOD mice as compared to BALB/c mice over time (Fig. 2G). Peripheral serum levels of eATP were then measured and were confirmed to be highest in 4-week-old NOD mice (Fig. 2H).

***T cells release eATP during an autoimmune response in vitro and eATP stimulates P2X7R expression on T cells***

We then assessed eATP release during an autoimmune response *in vitro* by incubating splenocytes from hyperglycemic NOD mice for 24 hours in the presence of different islet-derived peptides (BDC2.5, IGRP, GAD65 and insulin) in an ELISpot assay (Fig. 2I). eATP levels in the supernatant were increased during the autoimmune response against islet peptides and were observed to be highest following stimulation with the CD8-restricted peptide IGRP (Fig. 2I, red line). Interestingly, eATP levels paralleled the number of IFN- $\gamma$ <sup>+</sup> T cells generated during the autoimmune response (Fig. 2I, bar graph). To evaluate the effect of eATP on P2X7R expression in naïve T cells in *in vitro* studies, we used BzATP, a prototypic P2X7R agonist that exhibits 5- to 10-fold greater potency than ATP. CD4<sup>+</sup>CD25<sup>-</sup>

and CD8<sup>+</sup> T cells, isolated from normoglycemic NOD mice, were cultured for 24 hours in the presence of varying concentrations of activating cytokines, such as IL-1 $\beta$ , IL-6, TNF- $\alpha$ , MCP-1, ATP or BzATP, with P2X7R expression then quantified by flow cytometry. Almost all cytokines induced a slight but significant upregulation of P2X7R expression on CD4<sup>+</sup>CD25<sup>-</sup> T cells as compared to medium alone; in addition, a 3-fold increase in P2X7R expression was evident when culturing CD4<sup>+</sup>CD25<sup>-</sup> T cells with BzATP and ATP (Fig. 2J; Supplementary Fig. S2G). While no cytokines induced a significant increase in P2X7R expression in CD8<sup>+</sup> T cells, ATP and BzATP at its highest concentration significantly induced an increase in P2X7R expression as compared to medium alone (Fig. 2K; Supplementary Fig. S2H). It is likely that inflammation triggered by cytokines vs. cell necrosis involve two different pathways, such that only inflammation due to cell necrosis is eATP/P2X7R-dependent.

#### ***P2X7R<sup>+</sup> T cells increase in vivo and in vitro during the murine autoimmune response***

Flow cytometric analysis of splenic CD4<sup>+</sup> and CD8<sup>+</sup> T cells in NOD mice revealed an increased percentage of P2X7R<sup>+</sup>CD4<sup>+</sup> T cells, P2X7R<sup>+</sup>CD4<sup>+</sup> effector T cells and particularly P2X7R<sup>+</sup>CD8<sup>+</sup> T cells and P2X7R<sup>+</sup>CD8<sup>+</sup> effector T cells, both in 4- and partially in 10-week-old NOD mice as compared to hyperglycemic NOD mice (Fig. 2L-O). Conversely, the percentage of P2X7R<sup>+</sup> CD4<sup>+</sup>CD25<sup>+</sup>Foxp3<sup>+</sup> regulatory T cells (Tregs) was significantly increased in hyperglycemic NOD mice as compared to other groups (Fig. 2P). This observation led us to investigate the function of P2X7R<sup>pos</sup> and P2X7R<sup>neg</sup> Tregs. We thus compared the ability of P2X7R<sup>pos</sup> and P2X7R<sup>neg</sup> Tregs to suppress the autoimmune response generated by diabetogenic T cells isolated from NOD BDC2.5 mice and stimulated with BDC2.5 peptide. P2X7R<sup>pos</sup> Tregs showed impaired suppressive function (Supplementary Fig. S5A-B), reduced metabolic activity and lower oxygen consumption rates (OCR) as compared to P2X7R<sup>neg</sup> Tregs (Supplementary Fig. S5D-E). Moreover, P2X7R<sup>pos</sup> Tregs produced more pro-inflammatory cytokines (i.e. IFN- $\gamma$  and IL-17) compared to P2X7R<sup>neg</sup> Tregs (Supplementary Fig. S5C). P2X7R stimulation with BzATP during Treg generation also induced a decrease in the percentage of newly generated Tregs and

an overall reduction in FoxP3 expression (Supplementary Fig. S5F-H). Interestingly, P2X7R signaling with BzATP increased the production of proinflammatory cytokines (Supplementary Fig. S5I) as well as the percentage of apoptotic cells (Supplementary Fig. S5G).

When isolated CD4<sup>+</sup>CD25<sup>-</sup> and CD8<sup>+</sup> T cells were cultured for 24 hours in the presence of BDC2.5/IGRP peptides and CD11c<sup>+</sup> cells, a significant increase in P2X7R<sup>+</sup> cells, particularly in those that were CD8<sup>+</sup>, was evident (Fig. 2Q-R). Interestingly, islets from 4-week-old NOD mice showed preserved architecture and scanty T cell infiltrate with very few P2X7R<sup>+</sup> cells, while islets from 10-week-old and HgIc NOD exhibited substantial CD3<sup>+</sup> T cell infiltrate, which appeared to be predominantly P2X7R<sup>+</sup> (Fig. 3A-B and Supplementary Fig. S2A-B). We then evaluated the expression of P2XsR mRNA in the whole pancreas and in CD4<sup>+</sup>CD25<sup>-</sup> and CD8<sup>+</sup> T cells obtained from spleen of NOD mice at different ages. P2X1R and P2X7R mRNA expression appeared highest among P2X receptors in the pancreas of NOD mice in the early phase of the disease and decreased following islet infiltration and insulinitis (Fig. 3C). Conversely, mRNA P2X expression in splenic CD4<sup>+</sup>CD25<sup>-</sup> and CD8<sup>+</sup> T cells is broader and more diverse (Supplementary Fig. S2C-D). These data suggest that islet inflammation and damage that occurred during the autoimmune response contributes to the engagement of ATP/P2X7R immunity by stimulating P2X7R expression on T cells and thus creating a proinflammatory environment through generation of a pool of highly activated T cells committed to the Th1/Th17 lineage, which thus facilitates T1D onset.

***Targeting the eATP/P2X7R axis in vitro reduced T cell P2X7R expression as well as the CD8<sup>+</sup> T cell-dependent autoimmune response***

To evaluate whether targeting of eATP/P2X7R-driven immunity had any effect on the expression of P2X7R, isolated CD4<sup>+</sup>CD25<sup>-</sup> and CD8<sup>+</sup> T cells were cultured for 24 hours with different anti-cytokine monoclonal antibodies (mAbs) (i.e. anti-IFN- $\gamma$ , anti-IL-4 or anti-IL-17) or with P2X7R inhibitors (oATP and CE-224,535). Compared to baseline, CE-224,535, but not oATP, significantly reduced P2X7R

expression on both CD4<sup>+</sup>CD25<sup>-</sup> and CD8<sup>+</sup> T cells (Fig. 3D-E). A slight decrease was also observed in CD4<sup>+</sup>CD25<sup>-</sup> T cells cultured with anti-IFN- $\gamma$  mAb (Fig. 3D) and in CD8<sup>+</sup> T cells cultured with anti-IL-17 mAb (Fig. 3E). To test the effect of blocking eATP/P2X7R-driven immunity during an autoimmune response, we cultured splenocytes from hyperglycemic NOD mice with BDC2.5, IGRP, GAD65, and insulin peptides for 24 hours in the presence of different concentrations of oATP (1, 10, 100 $\mu$ M) in an ELISpot assay. Blocking the eATP/P2X7R axis reduced the production of IFN- $\gamma$  by T cells in this autoimmune assay (Fig. 3F). Interestingly, the effect was specific to P2X7R, as the P2X1R inhibitor NF449 and the P2X4R inhibitor 5-BDBD were ineffective or induced IFN- $\gamma$  production by T cells, respectively (Fig. 3G-H). We then cultured isolated CD4<sup>+</sup>CD25<sup>-</sup> and CD8<sup>+</sup> T cells in the same islet peptide-based ELISpot assay in the presence of different concentrations of oATP or CE-224,535, with islet peptides and CD11c<sup>+</sup> cells to present antigen. oATP, but not CE-224,535, reduced the production of IFN- $\gamma$  by CD8<sup>+</sup> T cells (Fig. 3K-L) but not by CD4<sup>+</sup>CD25<sup>-</sup> T cells (Fig. 3I-J) following stimulation with IGRP or BDC2.5 peptides, respectively. Interestingly, in the same aforementioned autoimmune assay, BzATP significantly reduced the number of IFN- $\gamma$ <sup>+</sup> T cells by inducing T cell apoptosis when used at higher concentrations (Supplementary Fig. S2E-F). In order to understand the effect of P2X7R targeting on a broader CD8<sup>+</sup>-restricted immune response, CD8<sup>+</sup> T lymphocytes isolated from peripheral blood of healthy control individuals were incubated with a mixture of vaccine antigens (Diftavax) for 24 hours in the presence or absence of P2X7R antagonists (oATP or CE224,535). The number of IFN- $\gamma$ -producing CD8<sup>+</sup> cells was significantly reduced after addition of both antagonists, reaffirming the effect of P2X7R targeting on CD8 activation (Supplementary Fig. S1F).

### ***Targeting the eATP/P2X7R axis delays diabetes onset in NOD mice in vivo***

We then tested the effect of targeting the eATP/P2X7R axis in NOD mice *in vivo* in early and late prevention of diabetes as well as in reversal studies, using (i) oATP, (ii) CE-224,535, and (iii) a combination of oATP or CE-224,535 with clinical-grade-dose Rapamycin. A significant delay in

diabetes onset in early prevention studies was observed in NOD mice treated with oATP or the combination of oATP and Rapamycin, but not in untreated controls or those treated with CE-224,535 alone or in combination with Rapamycin (Fig. 4A-D). In late prevention studies, both oATP and CE-224,535 successfully delayed diabetes onset when used in combination with Rapamycin but not when used alone (Fig. 4E-H). Treatment with Rapamycin alone did not show any effect on diabetes onset in either early or late prevention studies. In reversal studies, NOD mice treated with oATP alone, Rapamycin alone, or the combination of CE-224,535 and Rapamycin remained hyperglycemic (Supplementary Fig. S3A-E). The combination of oATP and Rapamycin or CE-224,535 alone resulted in 2 out of 5 mice becoming normoglycemic for several days, then reverting to hyperglycemia (Supplementary Fig. S3B-C). Rapamycin alone did not reverse hyperglycemia in NOD mice (Supplementary Fig. S3E). Histopathological analysis of 4-week-old NOD mice treated with oATP alone or in combination with Rapamycin demonstrated better preserved islet architecture and insulin staining as compared to untreated 4-week-old NOD mice (Fig. 4I). Diminished lymphoid infiltration was observed in the islets of mice treated with the combination of oATP plus Rapamycin as indicated by staining for the T cell marker CD3 when compared to both control animals and mice treated with oATP alone (Fig. 4I: 4-6). Semi-quantitative analysis confirmed the diminished islet infiltrate (Fig. 4K) despite a slight reduction in the number of islets of Langerhans in mice treated with either oATP alone or oATP and Rapamycin. The aforementioned effect may be related to Rapamycin, which has been reported to be capable of impairing islet cell function (Fig. 4L). Amelioration of islet architecture and of preserved insulin staining was also observed in 10-week-old NOD mice treated with the combination of oATP and Rapamycin in comparison to untreated and oATP-treated mice, despite the presence of lymphoid infiltrate (Fig. 4J). Thus, targeting the eATP/P2X7R axis delays diabetes onset in the early stages of the disease but does not revert established autoimmune diabetes, possibly because in the earlier disease stages, due to mild infiltration and greater available  $\beta$  cell mass, higher release of eATP by the islets

plays a role (Fig. 4A-D). At later stages of the disease, loss of  $\beta$  cell mass contributes to a decline in eATP release, which could explain the lack of effect when using eATP/P2X7R blocking agents (Fig. 4E-H). We then performed a series of autoimmune *in vitro* assays to mimic the onset of autoimmune diabetes observed in NOD mice.  $CD4^+CD25^-$  and  $CD8^+$  T cells thus were isolated from the spleens of NOD mice untreated or treated with oATP alone or in combination with Rapamycin, and cultured in the presence of BDC2.5 or IGRP peptides. The number of  $IFN-\gamma^+CD8^+$ , but not  $IFN-\gamma^+CD4^+$ , T cells was reduced in mice treated with oATP alone or in combination with Rapamycin as compared to untreated mice, suggesting an effect of P2X7R blockade on the  $CD8^+$  T cell-dependent autoimmune response only (Fig. 4M-N). Interestingly, when studying the  $P2X7R^{-/-}$  NOD mouse, which is not protected against autoimmune diabetes<sup>30</sup>, we observed substantial mRNA expression of P2X7R, while western blot analysis confirmed the absence of P2X7R expression on  $CD4^+CD25^-$  and  $CD8^+$  T cells (Fig. 4Q, S). Upregulation of other P2XRs expression on T cells was also evident (Fig. 4O-S). We then examined expression of CD38, a cyclic ADP ribose hydrolase that when absent in the NOD mouse, rapidly accelerates onset of hyperglycemia. Genetic deletion of P2X7R in CD38-deficient NOD mice was shown to prevent this rapid T1D onset<sup>30</sup>. Indeed, immunophenotypic expression analysis of splenocytes from  $P2X7R^{-/-}$  NOD revealed significant upregulation of CD38 expression on  $CD4^+$  and  $CD8^+$  T cells as compared to WT NOD (Supplementary Fig. S4A-D).

### ***Characterization of $P2X7R^{neg}$ and $P2X7R^{pos}$ T cells***

In order to further explore the role of the eATP/P2X7R pathway in T1D onset, we characterized  $P2X7R^{neg}$  and  $P2X7R^{pos}$  cells for migratory ability, autoimmune response and metabolic profile. Surprisingly, in NOD mice, T cells expressed a significant amount of intracellular P2X7R, which may serve as a P2X7R reservoir (Fig. 5A-D). Among  $CD4^+CD25^-$  T cells, those that were  $P2X7R^{neg}$  seemed to display enhanced migratory ability in response to SDF-1 as compared to  $P2X7R^{pos}$  (Fig. 5E). The opposite effect was observed in  $CD8^+$  T cells; those that were  $P2X7R^{pos}$  showed a significantly greater

migratory ability as compared to P2X7R<sup>neg</sup> (Fig. 5F), suggesting a differential impact of P2X7R signaling on CD4 and CD8 T cell migration ability. Moreover, P2X7R<sup>pos</sup> CD4<sup>+</sup>CD25<sup>-</sup> T cells and P2X7R<sup>pos</sup> CD8<sup>+</sup> T cells showed a significantly greater autoimmune response compared to P2X7R<sup>neg</sup> CD4<sup>+</sup>CD25<sup>-</sup> T cells and P2X7R<sup>neg</sup> CD8<sup>+</sup> T cells, as demonstrated by a substantially greater number of IFN- $\gamma$ <sup>+</sup> T cells generated by P2X7R<sup>pos</sup> CD4<sup>+</sup>CD25<sup>-</sup> T cells and P2X7R<sup>pos</sup> CD8<sup>+</sup> T cells during an islet peptide-based ELISpot assay (Fig. 5G-H). In addition, metabolic profiles were significantly altered between P2X7R<sup>pos</sup> CD4<sup>+</sup>CD25<sup>-</sup> T cells, P2X7R<sup>pos</sup> CD8<sup>+</sup> T cells, and their P2X7R<sup>neg</sup> counterparts. Upon examination of bioenergetic changes in the aforementioned four populations, the oxygen consumption rate (OCR), an indicator of oxidative phosphorylation (OXPHOS), was significantly decreased in the basal state in P2X7R<sup>pos</sup> CD4<sup>+</sup>CD25<sup>-</sup> T cells when compared to P2X7R<sup>neg</sup> CD4<sup>+</sup>CD25<sup>-</sup> T cells and P2X7R<sup>pos</sup> CD8<sup>+</sup> T cells (Fig. 5I-L). P2X7R<sup>pos</sup> CD4<sup>+</sup> T cells showed significantly reduced maximal respiration in response to the uncoupling agent FCCP, as compared to P2X7R<sup>neg</sup> CD4<sup>+</sup> T cells (Fig. 5I-J). While P2X7R<sup>pos</sup> CD8<sup>+</sup> T cells appeared hypermetabolic given that they showed significantly higher maximal respiration in response to the uncoupling agent FCCP, OCR values significantly increased in response to oligomycin (ATP synthase inhibitor), and to rotenone (complex I inhibitor) and antimycin A (complex III inhibitor), (Fig. 5J, L). The latter suggests differential behavior when mitochondrial respiration is augmented as spare respiratory capacity (SRC) increased in P2X7R<sup>pos</sup> CD8<sup>+</sup> T cells in comparison to their P2X7R<sup>neg</sup> counterparts (Fig. 5J, L). We have extended our investigation to assess the glycolytic capacity of P2X7R<sup>neg</sup> and P2X7R<sup>pos</sup> CD8<sup>+</sup> T cells. P2X7R<sup>neg</sup> CD8<sup>+</sup> T cells did not display a robust glycolytic response when exposed to glucose or oligomycin (Supplementary Fig. S3F-G) and therefore exhibited reduced glucose uptake, while P2X7R<sup>pos</sup> CD8<sup>+</sup> T cells displayed an increased glycolytic reserve, likely to enhance their activity during an autoimmune response (Supplementary Fig. S3F-G).

We then characterized P2X7R<sup>neg</sup> and P2X7R<sup>pos</sup> cells within CD4<sup>+</sup> T cells from NOD.BDC2.5 mice and

CD8<sup>+</sup> T cells from NOD.8.3 mice. Immunophenotypic analysis, examination of migratory properties, results of ELISpot assays and bioenergetic profiling confirmed what was observed for WT NOD mice (Fig. 5M-X), with minor differences. P2X7R<sup>pos</sup> CD4<sup>+</sup>CD25<sup>-</sup> T cells from NOD.BDC2.5 mice exhibited higher OCR at basal conditions and in response to FCCP (Fig. 5U,W), as well as higher ATP production (Fig. 5W) overall.

### ***The novel recombinant protein sP2X7R reduces CD8-restricted autoimmune responses***

We generated a recombinant protein based on the 595-amino-acid P2X7R extracellular domain (sP2X7R) (Fig. 6A-C), thus offering a novel therapeutic option able to quench eATP (Video S1). The addition of sP2X7R to an anti-islet peptide-based ELISpot reduced the number of IFN- $\gamma$ <sup>+</sup> CD8<sup>+</sup>, but not of CD4<sup>+</sup>, T cells from NOD mice (Fig. 6D-E). The same effect was observed when using transgenic CD8<sup>+</sup>/CD4<sup>+</sup> T cells (Fig. 6F-G). CD8<sup>+</sup> T cells that were cultured with IGRP peptide and sP2X7R exhibited higher OCR at basal conditions and in response to FCCP at all time points (Fig. 6H-I). ATP production was also higher in cells that were cultured with sP2X7R as compared to CD8<sup>+</sup> T cells cultured with IGRP peptide alone, suggesting interference of our recombinant protein sP2X7R with the eATP/P2X7R axis and with the bioenergetic activity of CD8<sup>+</sup> T cells (Fig. 6I). We can now propose a working hypothesis in which eATP released by  $\beta$  cells during stress/injury mediated by viruses, autoantibodies and other factors induces P2X7R expression on T cells (particularly on CD8<sup>+</sup> cells) and facilitates their activation, leading to T cell priming. Pharmacological targeting of the eATP/P2X7R signaling using oATP or the novel recombinant sP2X7R protein prevents the deleterious signaling that would be generated outright in CD8<sup>+</sup> autoreactive T cells, thus delaying the onset of diabetes (Fig. 6J).

## **Discussion**

The emerging role of eATP as an initiator of the immune response, aside from its metabolic function, has been the focus of intense investigation<sup>1,24</sup>. eATP levels can increase as a consequence of release from

damaged cells or by activated immune cells and can be sensed by P2X7R<sup>1,24</sup>, which is expressed on T cells, thereby triggering their activation. Our initial observation, described herein, that two P2X7R loss-of-function non-synonymous SNPs appear to be protective against T1D prompted us to hypothesize that eATP/P2X7R signaling may be involved in the onset of T1D, despite the lack of protection observed in P2X7R<sup>-/-</sup> NOD mice. To this end, we reported an upregulation of CD38 and of other P2XsR on T cells from P2X7R<sup>-/-</sup> NOD, which may explain why the incidence of T1D was not altered by genetic deletion of P2X7R. In fact, lack of CD38 may impair calcium mobilization and immune function, while accelerating T1D onset in NOD mice, whereas lack of P2X7R may counteract this effect and stabilize calcium efflux and prevent the acceleration of T1D onset. Notably, the “rs7958311” loss-of-function mutation was shown to be associated with insulin resistance and impaired glucose tolerance in a cohort of T2D patients<sup>31</sup>. Because eATP is secreted with insulin<sup>25,26</sup>, we also hypothesize that  $\beta$  cells may participate in their own demise by secreting eATP as a consequence of injury and thus may activate leukocytes in an initial step of the T cell-mediated anti-islet autoimmune response. ATP release is not restricted to leukocytes, as it has been described that eATP is also secreted by platelet-dense granules, therefore providing a positive feedback mechanism<sup>32</sup>. It is possible that this pathway that potentiates platelet activation through nucleotide receptors (P2X1, P2Y1 and P2Y12) expressed on the platelet surface may be affected as well<sup>32</sup>.

Phenotypic analysis of P2X7R expression on different T cell populations in the periphery of patients with newly diagnosed T1D revealed many perturbations of the P2X7R-related phenotype. Interestingly, we demonstrated that during an autoimmune response *in vitro*, eATP is released in high amounts and that this release may upregulate P2X7R on T cells (particularly on CD8<sup>+</sup> cells), thus creating a vicious cycle that sustains the autoimmune response and making P2X7R an attractive target in T1D. Pancreatic islets exposed to high glucose or to inflammatory cytokines increasingly released eATP as well; these conditions are found frequently in pre-diabetes. Peripheral levels of eATP are increased in the early

phase of T1D onset in NOD mice, and similarly, P2X7R expression is increased on CD8<sup>+</sup> T cells. Most, if not all, of the T cells infiltrating the pancreas in NOD mice appeared to be P2X7R<sup>+</sup>, and P2X7R mRNA was increased in the pancreata of NOD mice. Of note, P2X7R blockade was effective in reducing CD8-restricted, but not CD4-restricted, autoimmune responses *in vitro*. Targeting of eATP-P2X7R-driven immunity with oATP delayed diabetes onset in early prevention studies in NOD mice *in vivo*, with pathology confirming reduced lymphoid infiltrate and preserved insulin staining in treated NOD mice. Characterization of the P2X7R<sup>neg</sup> and P2X7R<sup>pos</sup> cellular compartments revealed that CD8<sup>+</sup>P2X7R<sup>+</sup> T cells migrate more efficiently and produce more IFN- $\gamma$ /IL-17 when challenged with islet peptides as compared to CD8<sup>+</sup>P2X7R<sup>neg</sup> T cells and, generally, as compared to CD4<sup>+</sup>CD25<sup>-</sup> cells. The bioenergetic profiles of P2X7R<sup>neg</sup> or P2X7R<sup>pos</sup> CD4<sup>+</sup>CD25<sup>-</sup> and CD8<sup>+</sup> T cells were significantly different. Although it has been reported that non-obese diabetic (NOD) mice develop an aggressive T cell-mediated destruction of  $\beta$  cells with limited similarity to human disease and also show poor predictive value in screening for effective intervention therapies for T1D, the NOD mouse remains the most reliable T1D model, as it shares many genetic and physio-pathological features with human T1D<sup>33</sup>. The secretion of eATP and insulin constitute, *per se*, a potential driving force for T cell activation. Any perturbation of insulin secretion, or any overexertion by or stress of  $\beta$  cells, may favor increased release of eATP, which in turn may activate passenger leukocytes. Viral infection and endoplasmic reticulum stress may result in perturbation of the eATP-releasing machinery within  $\beta$  cells as well. Second, it appears that autoreactive CD8<sup>+</sup> T cells are more prone to be affected by and possibly more dependent upon eATP/P2X7R signaling as compared to autoreactive CD4<sup>+</sup> T cells. Third and finally, the novel recombinant protein sP2X7R, which we created and produced based on the extracellular domain of P2X7R, reduced CD8<sup>+</sup> T cell activity and autoimmune responses and thus may represent a novel therapeutic tool for the prevention of T1D. In conclusion, eATP/P2X7R signaling facilitates the onset of

autoimmune diabetes by fueling autoreactive CD8<sup>+</sup> cells and may represent a novel therapeutic target for T1D.

### **Author contributions**

S.T. designed and performed experiments, analyzed data, and wrote the paper; C.F. and A.P. designed and performed research, analyzed the data, and edited the paper; M.BN., A.V., F.D, V.U., S.F., R.B., S.D., C.R., A.M., E.F. performed experiments and analyzed data; A.S., D.C., E.G., C.M., F.B., M.G.P., C.H.W. helped with sample collection, pathology and analysis of data; C.R., F.F., F.D.V., S.D., A.P. G.V.Z., C.W., M.AA. coordinated research; P.F. conceived the study, designed research, wrote and edited the paper. All authors reviewed and edited the paper.

### **Acknowledgments**

Paolo Fiorina is the recipient of an EFSD/Sanofi European Research Programme and is supported by an American Heart Association (AHA) Grant-in-Aid. We thank the Fondazione Romeo and Enrica Invernizzi for their generous support.

Dr. Paolo Fiorina is the guarantor of this work and, as such, had full access to all the data in the study and takes responsibility for the integrity of the data and the accuracy of the data analysis.

### **Disclaimer**

This article was prepared while Dr. Pileggi was employed at the University of Miami. He is currently employed at the Center for Scientific Review of the National Institutes of Health. The opinions expressed in this article are the author's own and do not necessarily reflect the views of the National Institutes of Health, the Department of Health and Human Services, or the United States government.

## Disclosure

The authors have nothing to disclose.

## References

1. Vergani A, Tezza S, D'Addio F, et al. Long-term heart transplant survival by targeting the ionotropic purinergic receptor P2X7. *Circulation* 2013;127:463-75.
2. Guleria I, Gubbels Bupp M, Dada S, et al. Mechanisms of PDL1-mediated regulation of autoimmune diabetes. *Clin Immunol* 2007;125:16-25.
3. McClymont SA, Putnam AL, Lee MR, et al. Plasticity of human regulatory T cells in healthy subjects and patients with type 1 diabetes. *J Immunol* 2011;186:3918-26.
4. Fiorina P, Jurewicz M, Vergani A, et al. Targeting the CXCR4-CXCL12 axis mobilizes autologous hematopoietic stem cells and prolongs islet allograft survival via programmed death ligand 1. *J Immunol* 2011;186:121-31.
5. Naserke HE, Bonifacio E, Ziegler AG. Prevalence, characteristics and diabetes risk associated with transient maternally acquired islet antibodies and persistent islet antibodies in offspring of parents with type 1 diabetes. *J Clin Endocrinol Metab* 2001;86:4826-33.
6. Lind M, Svensson AM, Kosiborod M, et al. Glycemic control and excess mortality in type 1 diabetes. *N Engl J Med* 2014;371:1972-82.
7. Fiorina P, Shapiro AM, Ricordi C, Secchi A. The clinical impact of islet transplantation. *Am J Transplant* 2008;8:1990-7.
8. D'Addio F, Maffi P, Vezzulli P, et al. Islet transplantation stabilizes hemostatic abnormalities and cerebral metabolism in individuals with type 1 diabetes. *Diabetes Care* 2014;37:267-76.
9. Fiorina P, Secchi A. Pancreatic islet cell transplant for treatment of diabetes. *Endocrinol Metab Clin North Am* 2007;36:999-1013; ix.

10. Novak I. ATP as a signaling molecule: the exocrine focus. *News Physiol Sci* 2003;18:12-7.
11. Elliott MR, Chekeni FB, Trampont PC, et al. Nucleotides released by apoptotic cells act as a find-me signal to promote phagocytic clearance. *Nature* 2009;461:282-6.
12. Schenk U, Westendorf AM, Radaelli E, et al. Purinergic control of T cell activation by ATP released through pannexin-1 hemichannels. *Sci Signal* 2008;1:ra6.
13. Piccini A, Carta S, Tassi S, Lasiglie D, Fossati G, Rubartelli A. ATP is released by monocytes stimulated with pathogen-sensing receptor ligands and induces IL-1beta and IL-18 secretion in an autocrine way. *Proc Natl Acad Sci U S A* 2008;105:8067-72.
14. Ralevic V, Burnstock G. Receptors for purines and pyrimidines. *Pharmacol Rev* 1998;50:413-92.
15. Khakh BS, North RA. P2X receptors as cell-surface ATP sensors in health and disease. *Nature* 2006;442:527-32.
16. Wilhelm K, Ganesan J, Muller T, et al. Graft-versus-host disease is enhanced by extracellular ATP activating P2X7R. *Nat Med* 2010;16:1434-8.
17. Junger WG. Immune cell regulation by autocrine purinergic signalling. *Nat Rev Immunol* 2011;11:201-12.
18. Casati A, Frascoli M, Traggiati E, Proietti M, Schenk U, Grassi F. Cell-autonomous regulation of hematopoietic stem cell cycling activity by ATP. *Cell Death Differ* 2011;18:396-404.
19. Gabel CA. P2 purinergic receptor modulation of cytokine production. *Purinergic Signal* 2007;3:27-38.
20. Atarashi K, Nishimura J, Shima T, et al. ATP drives lamina propria T(H)17 cell differentiation. *Nature* 2008;455:808-12.
21. Yip L, Woehrle T, Corriden R, et al. Autocrine regulation of T-cell activation by ATP release and P2X7 receptors. *FASEB J* 2009;23:1685-93.

22. Ferrari D, Pizzirani C, Adinolfi E, et al. The P2X7 receptor: a key player in IL-1 processing and release. *J Immunol* 2006;176:3877-83.
23. Vergani A, Fotino C, D'Addio F, et al. Effect of the purinergic inhibitor oxidized ATP in a model of islet allograft rejection. *Diabetes* 2013;62:1665-75.
24. Vergani A, Tezza S, Fotino C, et al. The Purinergic System in Allotransplantation. *Am J Transplant* 2014.
25. Richards-Williams C, Contreras JL, Berecek KH, Schwiebert EM. Extracellular ATP and zinc are co-secreted with insulin and activate multiple P2X purinergic receptor channels expressed by islet beta-cells to potentiate insulin secretion. *Purinergic Signal* 2008;4:393-405.
26. Geisler JC, Corbin KL, Li Q, Feranchak AP, Nunemaker CS, Li C. Vesicular nucleotide transporter-mediated ATP release regulates insulin secretion. *Endocrinology* 2013;154:675-84.
27. Murgia M, Hanau S, Pizzo P, Rippla M, Di Virgilio F. Oxidized ATP. An irreversible inhibitor of the macrophage purinergic P2Z receptor. *J Biol Chem* 1993;268:8199-203.
28. Rizzo R, Ferrari D, Melchiorri L, et al. Extracellular ATP acting at the P2X7 receptor inhibits secretion of soluble HLA-G from human monocytes. *J Immunol* 2009;183:4302-11.
29. Falzoni S, Donvito G, Di Virgilio F. Detecting adenosine triphosphate in the pericellular space. *Interface Focus* 2013;3:20120101.
30. Chen YG, Scheuplein F, Driver JP, et al. Testing the role of P2X7 receptors in the development of type 1 diabetes in nonobese diabetic mice. *J Immunol* 2011;186:4278-84.
31. Todd JN, Poon W, Lyssenko V, et al. Variation in glucose homeostasis traits associated with P2RX7 polymorphisms in mice and humans. *J Clin Endocrinol Metab* 2015;100:E688-96.
32. Kahner BN, Shankar H, Murugappan S, Prasad GL, Kunapuli SP. Nucleotide receptor signaling in platelets. *J Thromb Haemost* 2006;4:2317-26.

33. Roep BO, Atkinson M. Animal models have little to teach us about type 1 diabetes: 1. In support of this proposal. *Diabetologia* 2004;47:1650-6.

## TABLE AND FIGURE LEGENDS

**Table 1.** Baseline demographic characteristics of patients enrolled. Data are expressed as mean  $\pm$  SEM.

	Healthy Donors (n=10)	Long-term T1D (n=10)	Newly diagnosed T1D (n=10)	T2D (n=5)	P values
Sex (n) Male/Female	4/6	4/6	5/5	4/1	NS
Age (Years)	42.0 $\pm$ 5.0	42.0 $\pm$ 12.3	10.2 $\pm$ 3.2	57.2 $\pm$ 1.7	<i>P</i> <0.001
Diabetes duration (Years)	-	27.1 $\pm$ 8.5	-	3.4 $\pm$ 0.9	N/A
HbA1c (%) [mmol/mol]	5.3 $\pm$ 1.0 [34 $\pm$ 10.9]	8.3 $\pm$ 1.1 [67 $\pm$ 12.0]	12.2 $\pm$ 1.4 [110 $\pm$ 14.8]	6.3 $\pm$ 0.2 [45.4 $\pm$ 2.9]	<i>P</i> <0.001 <i>P</i> <0.001
EIR (UI)	-	39.8 $\pm$ 10.0	-	-	N/A

**Abbreviations.** Number (n); SEM (standard error of the mean); T1D (type 1 diabetes); T2D (type 2 diabetes); HbA1c (%) (glycated hemoglobin A1c %); EIR (exogenous insulin requirement); not significant (NS); not applicable (N/A) .

**Figure 1. The eATP/P2X7R axis plays a role in human T1D onset.** (A, B) The human *P2X7R* SNP distribution among the GoKind and ESP6500EA cohorts is shown. Two loss-of-function mutations (rs3751143 and rs7958311) appeared to be protective toward the onset of T1D (rs3751143: odds ratio [OR]=0.8; rs7958311: OR=0.86) even after a conservative Bonferroni correction. (C) Increased eATP release by PBMCs from T1D patients was observed following IA-2 challenge as compared to PBMCs alone; Pediacel was used as a positive control. (D-S) Greater numbers of P2X7R<sup>+</sup>CD4<sup>+</sup> T cells (D-E), P2X7R<sup>+</sup>CD4<sup>+</sup>CD45RO<sup>+</sup>CCR7<sup>+</sup> effector memory T cells (F-G), P2X7R<sup>+</sup>CD8<sup>+</sup> T cells (L-M) and, to a lesser extent, P2X7R<sup>+</sup>CD8<sup>+</sup>CD45RO<sup>+</sup>CCR7<sup>-</sup> central memory T cells (P-Q) were evident in long-standing T1D patients as compared to healthy controls, T2D patients and newly diagnosed T1D patients. Increased numbers of P2X7R<sup>+</sup>CD4<sup>+</sup>CD45RO<sup>+</sup>CCR7<sup>-</sup> central memory T cells (H-I), P2X7R<sup>+</sup>CD8<sup>+</sup>CD45RO<sup>+</sup>CCR7<sup>+</sup> effector memory T cells (N-O) and P2X7R<sup>+</sup>CD8<sup>+</sup>CD45RO<sup>+</sup>CCR7<sup>-</sup> central memory T cells (P-Q) were observed in newly diagnosed T1D patients as compared to healthy controls, T2D patients and long-standing T1D patients, respectively. No difference or only slight differences were observed in the numbers of P2X7R<sup>+</sup>CD19<sup>+</sup> (J-K), and P2X7R<sup>+</sup>CD11c<sup>+</sup> (R-S) cells among groups. (T) oATP and CE-224,535 inhibited the anti-islet immune response following culture of PBMCs from new onset T1D patients with the IA-2 peptide; Pediacel was used as a positive control. (U-X) While within the CD4<sup>+</sup>CD25<sup>-</sup> T cell population the increased percentage of IFN- $\gamma$ <sup>+</sup> and IL-17<sup>+</sup> cells during the autoimmune response to IA-2 peptide was observed in the P2X7R<sup>neg</sup> subpopulation (U-V), for CD8<sup>+</sup> T cells most IL-17<sup>+</sup> cells generated during the autoimmune response to IA-2 peptide were within the P2X7R<sup>pos</sup> subpopulation (W-X). Data are expressed as mean $\pm$ standard error of the mean (SEM). Data are representative of at least n=3 samples. \**P*<0.05; \*\**P*<0.01; \*\*\**P*<0.001.

**Abbreviations.** nsSNP (non-synonymous single nucleotide polymorphisms); ESP6500EA (Exome Sequencing Project 6500 European American); PBMCs (peripheral blood mononuclear cells); GoKinD (Genetics of Kidneys in Diabetes); OR (odds ratio); eATP (extracellular ATP); oATP (oxidized ATP).

**Figure 2.  $\beta$  cells release eATP during stress.** (A, B) A glucose-dependent increase in the extent of luminescence (A) was evident in pancreata harvested from pmeLUC transgenic mice, cultured in the presence of different glucose concentrations and quantified as photons/seconds/grams of pancreas (B). (C) Higher levels of eATP were found in the supernatants of murine islets obtained from 10-week-old NOD/SCID mice and cultured in high glucose at different time points as compared to controls. The same effect was evident to a lesser extent with a cocktail of cytokines (IL-1 $\beta$ , TNF- $\alpha$  and IFN- $\gamma$ ), with high glucose being the more robust inducer of eATP. (D) High-glucose conditions and cytokines (IL-1 $\beta$ , TNF- $\alpha$  and IFN- $\gamma$ ) caused release of eATP by human islets cultured for 60 minutes. (E-G) A stable luminescence signal, as a proxy for *in vivo* eATP release, was observed in BALB/c mice injected i.p. with HEK293-pmeLUC transgenic cells and D-luciferin at different ages, while in NOD mice the luminescence signal appeared higher than in BALB/c mice. A gradual disappearance of bioluminescence was evident over time in NOD mice, paralleling the autoimmune-mediated destruction of pancreatic islets. (H) Higher levels of eATP in peripheral serum were detected in 4-week-old NOD mice, and in hyperglycemic NOD mice to a lesser extent, as compared to 10-week-old NOD mice. (I) During islet peptide (BDC2.5, IGRP, GAD65 and insulin) (red line) stimulation of splenocytes from NOD mice, IGRP (a CD8-restricted islet peptide) caused the highest release of eATP in the supernatant and the highest increase in the number of IFN- $\gamma$ <sup>+</sup> cells as compared to controls. BDC2.5, GAD65 and insulin peptide stimulation induced an increase in the number of IFN- $\gamma$ <sup>+</sup> spots as compared to controls as well, but to a lesser extent. (J, K) CD4<sup>+</sup>CD25<sup>-</sup> T cells cultured in the presence of different concentrations of IL-1 $\beta$ , IL-6, TNF- $\alpha$ , MCP-1 or BzATP showed a slight but significant upregulation of P2X7R expression on CD4<sup>+</sup>CD25<sup>-</sup> T cells, while in CD8<sup>+</sup> T cells, BzATP only was capable of upregulating P2X7R expression. (L-P) In 4-week-old NOD mice, the percentages of P2X7R<sup>+</sup> on CD4<sup>+</sup>/CD4<sup>+</sup> effector T cells and CD8<sup>+</sup>/CD8<sup>+</sup> effector T cells were increased as compared to 10-week-old Nglc or >14-week-

old Hglc NOD mice. P2X7R<sup>+</sup>CD4<sup>+</sup> effector, P2X7R<sup>+</sup>CD8<sup>+</sup> and CD8<sup>+</sup> effector T cells were increased in 10-week-old mice as compared to hyperglycemic NOD. The percentage of P2X7R<sup>pos</sup> Tregs was increased in hyperglycemic as compared to 4- and 10-week-old NOD mice and in 4- as compared to 10-week-old NOD mice (**Q-R**). P2X7R expression was increased in CD8<sup>+</sup> T cells and in CD4<sup>+</sup>CD25<sup>-</sup> T cells, to a lesser extent, after culture with BDC2.5 and IGRP peptides respectively. (**S**) Insulinitis score in 4-week-old, 10-week-old and hyperglycemic NOD mice is shown; n=9 sections per group were analyzed. Data are expressed as mean±standard error of the mean (SEM). Data are representative of at least n=3 mice. \**P*<0.05; \*\**P*<0.01; \*\*\**P*<0.001.

**Abbreviations.** eATP (extracellular ATP); HG (high glucose); wks (weeks of age); Nglc (normoglycemic); Hglc (hyperglycemic); AUC (area under the curve); BzATP (Benzoyl-ATP).

**Figure 3. P2X7R<sup>+</sup> T cells make up the vast majority of pancreas-infiltrating cells, while P2X7R blockade reduces the autoimmune response *in vitro*.** (**A, B**) Islets from 10- and, to a lesser extent, 4-week-old NOD mice showed CD3<sup>+</sup> T cell (green) infiltrate, which appeared to be predominantly P2X7R<sup>+</sup> (red). (**C**) P2X1R, P2X4R and P2X7R mRNA pancreatic expression was evident in 4- and, to a lesser extent, 10-week-old NOD mice. (**D**) Significant downregulation of P2X7R expression on CD4<sup>+</sup>CD25<sup>-</sup> T cells was observed when cells were cultured with anti-IFN- $\gamma$  or the P2X7R inhibitor CE-224,535 as compared to medium alone. (**E**) P2X7R downregulation was observed on CD8<sup>+</sup> T cells cultured with anti-IL-17 or CE-224,535 as compared to medium alone. (**F**) Splenocytes from hyperglycemic NOD mice cultured with the CD4/CD8-restricted islet mimotope peptides BDC2.5/IGRP respectively or with GAD65 and insulin in the presence of oATP showed a reduction in the number of IFN- $\gamma$ <sup>+</sup> T cells as compared to controls. (**G-H**) Splenocytes from hyperglycemic NOD mice cultured with BDC2.5 or IGRP peptides in the presence of different concentrations of the P2X1R antagonist NF449 or the P2X4R antagonist 5-BDBD did not show any effect or showed an increase in the number of IFN- $\gamma$ <sup>+</sup> T cells,

respectively. **(I-L)** oATP, but not CE-224,535, reduced the number of IFN- $\gamma^+$  CD8 $^+$ , but not CD4 $^+$ , T cells when CD4 $^+$ CD25 $^-$  cells isolated from BDC2.5 TCR Tg NOD mice **(I-J)** or CD8 $^+$  T cells isolated from 8.3 TCR Tg NOD mice **(K-L)** were cultured with BDC2.5 or IGRP peptides, respectively, in the presence of different concentrations of oATP or CE-224,535. Data are expressed as mean $\pm$ standard error of the mean (SEM). Data are representative of at least n=3 mice: \* $P$ <0.05; \*\* $P$ <0.01; \*\*\* $P$ <0.001.

**Abbreviations.** wks (weeks of age); Nglc (normoglycemic); Hglc (hyperglycemic); H&E (hematoxylin and eosin); oATP (oxidized ATP).

**Figure 4. P2X7R blockade delays diabetes in NOD mice and reduces islet infiltration and the autoimmune response by CD8 $^+$  cells.** **(A-H)** The effect of P2X7R blockade was tested in early (4-week-old NOD mice) and late (10-week-old NOD mice) prevention studies *in vivo* using (i) oATP, (ii) CE-224,535, and (iii) a combination of oATP or CE-224,535 with clinical-grade-dose Rapamycin. The treatment with oATP and oATP plus Rapamycin, but not with CE-224,535 alone or with Rapamycin, significantly delayed the onset of diabetes in the early prevention study setting as compared to untreated animals **(A, B)**; data are representative of n=10 mice per group. In the late prevention study, while oATP and CE-224,535 alone did not show any effect on the onset of diabetes **(E and G)**, their combination with Rapamycin successfully delayed diabetes onset **(F and H)**; data are representative of n=10 mice per group. **(I, J)** Representative H&E staining and immunohistochemical analysis of pancreatic islet tissue sections from the different groups of treated and untreated NOD mice. **(K and L)** Semi-quantitative analysis of islet infiltrate in 4-week-old treated NOD mice revealed that oATP+Rapamycin is more effective in reducing islet infiltration, although it is associated with an overall reduced number of islets. **(M, N)** CD4 $^+$ CD25 $^-$  and CD8 $^+$  T cells isolated from the spleens of 10-week-old treated and untreated NOD mice and cultured in the presence of BDC2.5 or IGRP peptides respectively showed a reduced number of IFN- $\gamma^+$  CD8 $^+$ , but not CD4 $^+$ , T cells in mice treated with oATP alone or in combination with

Rapamycin as compared to untreated mice. **(O)** The pancreata of 10-week-old normoglycemic P2X7R<sup>-/-</sup> and WT NOD mice contain P2X7R mRNA. **(P)** mRNA expression of P2X1R, P2X2R, P2X4R, P2X5R and P2X7R in splenic CD4<sup>+</sup>CD25<sup>-</sup> cells were significantly increased in P2X7R<sup>-/-</sup> NOD mice as compared to WT NOD mice; **(Q)** Western blot analysis of P2X1R, P2X4R and P2X7R in splenic CD4<sup>+</sup>CD25<sup>-</sup> T cells confirmed the absence of P2X7R protein in P2X7R<sup>-/-</sup> NOD mice as compared to WT NOD mice. **(R)** mRNA expression of P2X1R, P2X4R, P2X5R and P2X7R in splenic CD4<sup>+</sup>CD25<sup>-</sup> and in CD8<sup>+</sup> T cells (except for P2X2R) were significantly increased in P2X7R<sup>-/-</sup> NOD mice as compared to WT NOD mice; **(S)** Western blot analysis of P2X1R, P2X4R and P2X7R in splenic CD8<sup>+</sup> T cells confirming the absence of P2X7R protein in P2X7R<sup>-/-</sup> NOD mice as compared to WT NOD mice. Data are expressed as mean±standard error of the mean (SEM). Data are representative of at least n=3 mice. \**P*<0.05; \*\**P*<0.01; \*\*\**P*<0.001.

**Abbreviations.** H&E (hematoxylin and eosin); oATP (oxidized ATP); Rapa (Rapamycin); A.U. (Arbitrary Units).

**Figure 5. Characterization of P2X7R<sup>neg</sup> and P2X7R<sup>pos</sup> cells reveals dependence of CD8 T cells on eATP/P2X7R signaling.** **(A-D)** P2X7R<sup>neg</sup> CD4<sup>+</sup>CD25<sup>-</sup>/CD8<sup>+</sup> T cells isolated from 10-week-old hyperglycemic or normoglycemic NOD or BDC2.5/8.3 TCR Tg NOD mice (n=3 samples per group) showed no surface expression of P2X7R, while significant intracellular expression was detected. **(E, F)** The percentage of P2X7R<sup>neg</sup> CD4<sup>+</sup>CD25<sup>-</sup> T cells migrating to SDF-1 was significantly higher as compared to P2X7R<sup>pos</sup> CD4<sup>+</sup>CD25<sup>-</sup> T cells, while the opposite was observed in CD8<sup>+</sup> T cells, with a higher percentage of migrating P2X7R<sup>pos</sup> CD8<sup>+</sup> T cells as compared to P2X7R<sup>neg</sup> CD8<sup>+</sup> T cells. **(G, H)** P2X7R<sup>pos</sup> CD4<sup>+</sup>CD25<sup>-</sup>/CD8<sup>+</sup> T cells from hyperglycemic NOD mice cultured with the CD4-/CD8-restricted islet mimotope peptides BDC2.5 and IGRP, respectively, generated more IFN-γ<sup>+</sup> T cells. **(I and K)** Higher OCR in basal conditions and after FCCP addition was observed in P2X7R<sup>neg</sup> CD4<sup>+</sup>CD25<sup>-</sup>

T cells as compared to P2X7R<sup>pos</sup> CD4<sup>+</sup>CD25<sup>-</sup> T cells. **(J and L)** In P2X7R<sup>pos</sup> CD8<sup>+</sup> T cells, OCR was increased after FCCP addition and reduced in response to rotenone/antimycin A as compared to P2X7R<sup>neg</sup> CD8<sup>+</sup> T cells. While the maximal respiration capacity and SRC of P2X7R<sup>pos</sup> CD8<sup>+</sup> T cells were significantly increased, following addition of oligomycin and in response to rotenone/antimycin A, the OCR was significantly reduced as compared to P2X7R<sup>pos</sup> CD8<sup>+</sup> T cells. **(M-P)** P2X7R<sup>neg</sup> CD4<sup>+</sup>CD25<sup>-</sup>/CD8<sup>+</sup> T cells from NOD.BDC2.5 and NOD.8.3 mice showed significant intracellular P2X7R expression as well. **(Q, R)** Among CD4<sup>+</sup>CD25<sup>-</sup> T cells from NOD.BDC2.5 mice, the percentage of migrating P2X7R<sup>neg</sup> cells was significantly higher as compared to P2X7R<sup>pos</sup> cells, while among CD8<sup>+</sup> T cells from NOD.8.3 mice, the percentage of P2X7R<sup>pos</sup> cells migrating was higher as compared to P2X7R<sup>neg</sup> cells. **(S, T)** Among both CD4<sup>+</sup>CD25<sup>-</sup> and CD8<sup>+</sup> T cells, the number of IFN- $\gamma$ <sup>+</sup> T cells generated during an islet peptide-based autoimmune assay was significantly higher among P2X7R<sup>pos</sup> as compared to the P2X7R<sup>neg</sup> cells. **(U and W)** Among CD4<sup>+</sup>CD25<sup>-</sup> T cells from NOD.BDC2.5 mice, an increase in OCR was observed in P2X7R<sup>pos</sup> cells in basal conditions and after FCCP injection as compared to P2X7R<sup>neg</sup> cells. Among CD4<sup>+</sup>CD25<sup>-</sup> T cells from NOD.BDC2.5 mice, the basal, maximal respiration and ATP-related OCR were significantly increased in P2X7R<sup>pos</sup> as compared to P2X7R<sup>neg</sup> cells. **(V and X)** Among CD8<sup>+</sup> T cells from NOD.8.3 mice, OCR was increased in basal conditions and after FCCP injection in P2X7R<sup>neg</sup> as compared to P2X7R<sup>pos</sup> cells. Among CD8<sup>+</sup> T cells from NOD.8.3 mice, the basal, maximal respiration, SRC and ATP-related OCR increased in P2X7R<sup>neg</sup> as compared to P2X7R<sup>pos</sup> cells. Data are expressed as mean $\pm$ standard error of the mean (SEM). Data are representative of at least n=3 mice. \* $P$ <0.05; \*\* $P$ <0.01; \*\*\* $P$ <0.001.

**Abbreviations.** OCR (oxygen consumption rate); FCCP (carbonyl cyanide p-trifluoromethoxyphenyl hydrazone); SRC (spare respiratory capacity).

**Figure 6. The novel recombinant protein sP2X7R containing the extracellular P2X7R domain**

**reduces the *in vitro* autoimmune response. (A, B)** A schematic representation of the sequence and domain arrangements of human P2X7R and sP2X7R. **(C)** SDS-PAGE of sP2X7R after purification by gel filtration and staining with Coomassie blue is shown. **(D, E)** CD4<sup>+</sup>CD25<sup>-</sup> and CD8<sup>+</sup> T cells isolated from hyperglycemic NOD mice were cultured with the BDC2.5 and the IGRP peptides respectively; 1μM sP2X7R reduces the number of IFN-γ<sup>+</sup>CD8<sup>+</sup>, but not CD4<sup>+</sup>, T cells. **(F, G)** CD4<sup>+</sup>CD25<sup>-</sup> and CD8<sup>+</sup> T cells isolated from NOD.BDC2.5/8.3 mice were cultured with BDC2.5 and IGRP peptides and sP2X7R. sP2X7R reduces the number of IFN-γ<sup>+</sup>CD4<sup>+</sup>/CD8<sup>+</sup> T cells dose-dependently. **(H, I)** Metabolic profile of CD8<sup>+</sup> T cells at steady state and during an autoimmune response with or without sP2X7R. T cells cultured with sP2X7R showed higher OCR at basal and after FCCP as compared to controls. Basal and non-mitochondrial respiration as well as ATP production levels were higher in cells cultured with sP2X7R as compared to controls. **(J)** Working hypothesis summarizing the role of the eATP/P2X7R axis in the onset of T1D and the effects of the novel sP2X7R recombinant protein. Data are expressed as mean±standard error of the mean (SEM). Data are representative of at least n=3 mice. \**P*<0.05; \*\**P*<0.01; \*\*\**P*<0.001.

**Abbreviations.** sP2X7R (soluble P2X7R); OCR (oxygen consumption rate); FCCP (carbonyl cyanide p-trifluoromethoxyphenyl hydrazone).

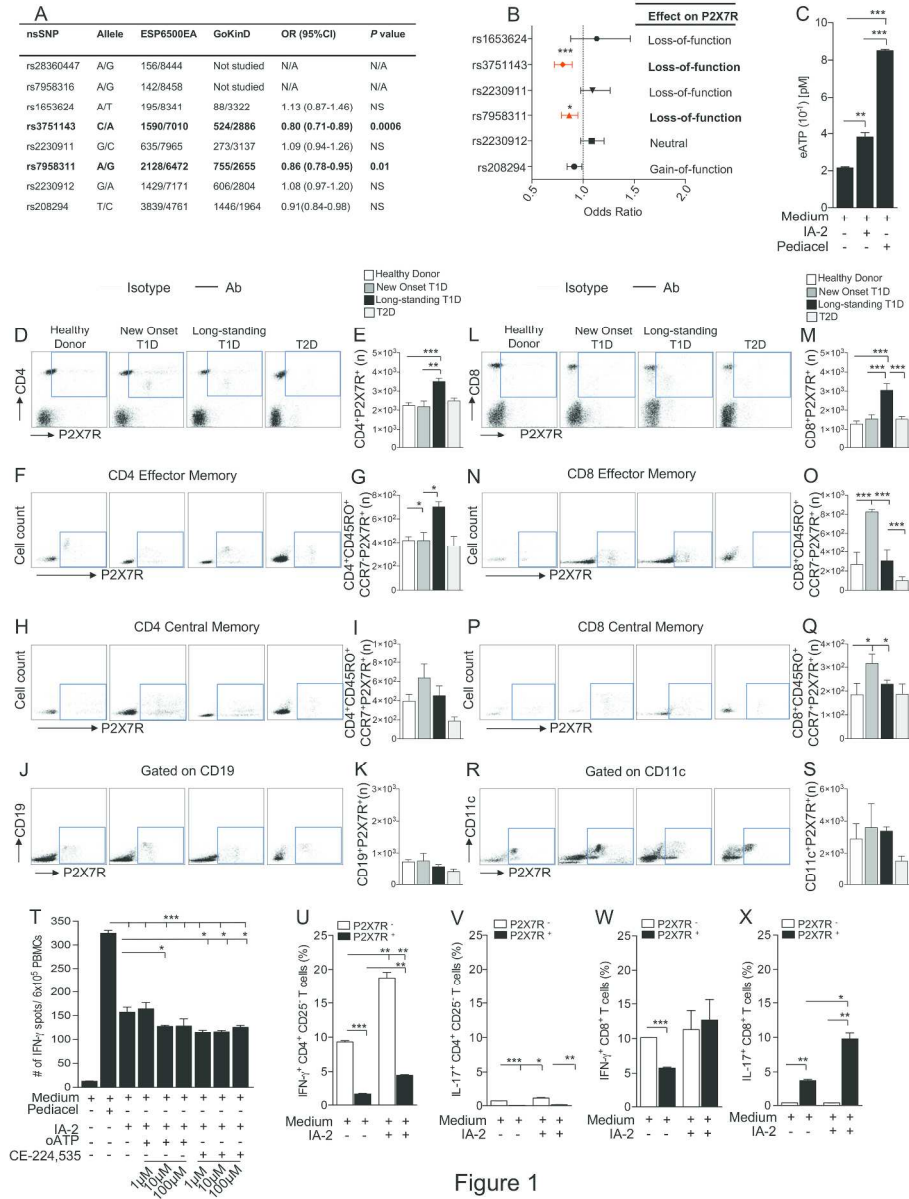


Figure 1

Figure 1

270x361mm (300 x 300 DPI)

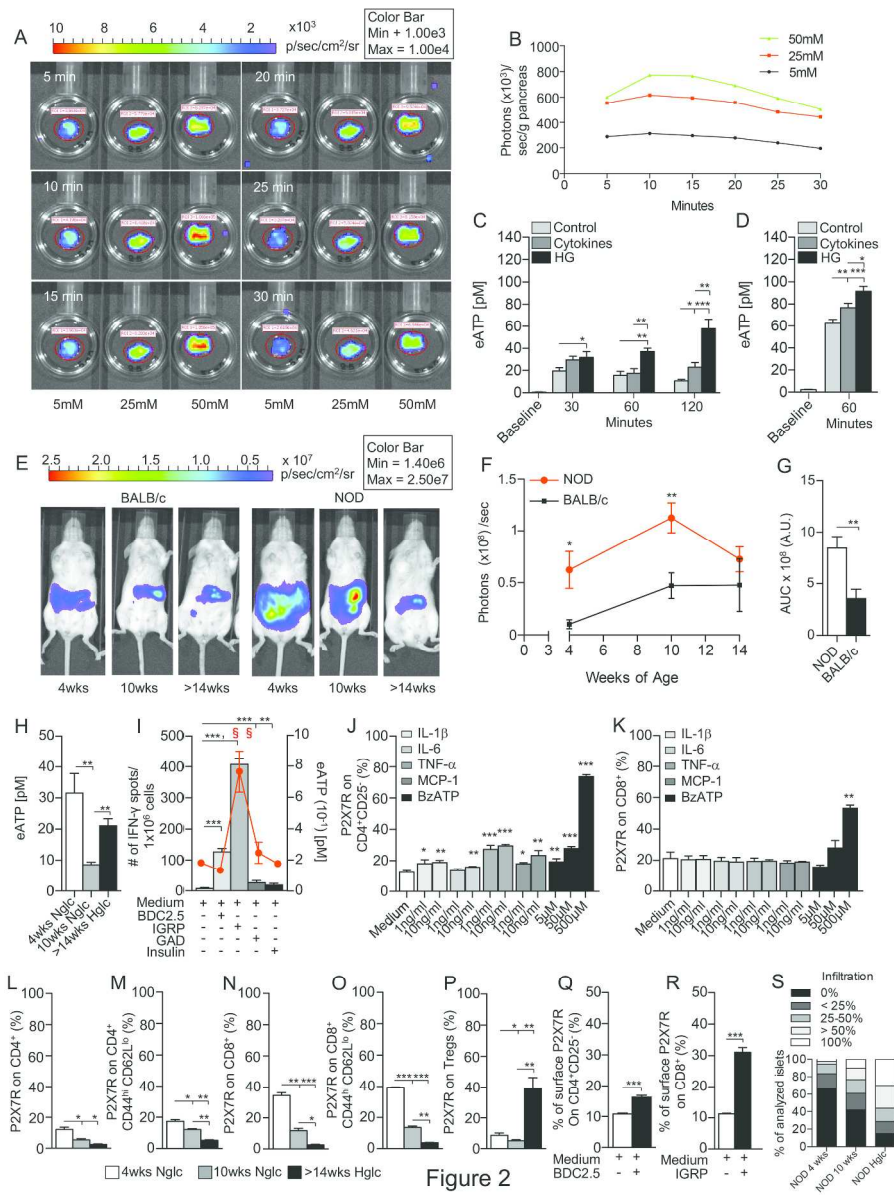


Figure 2

270x361mm (300 x 300 DPI)

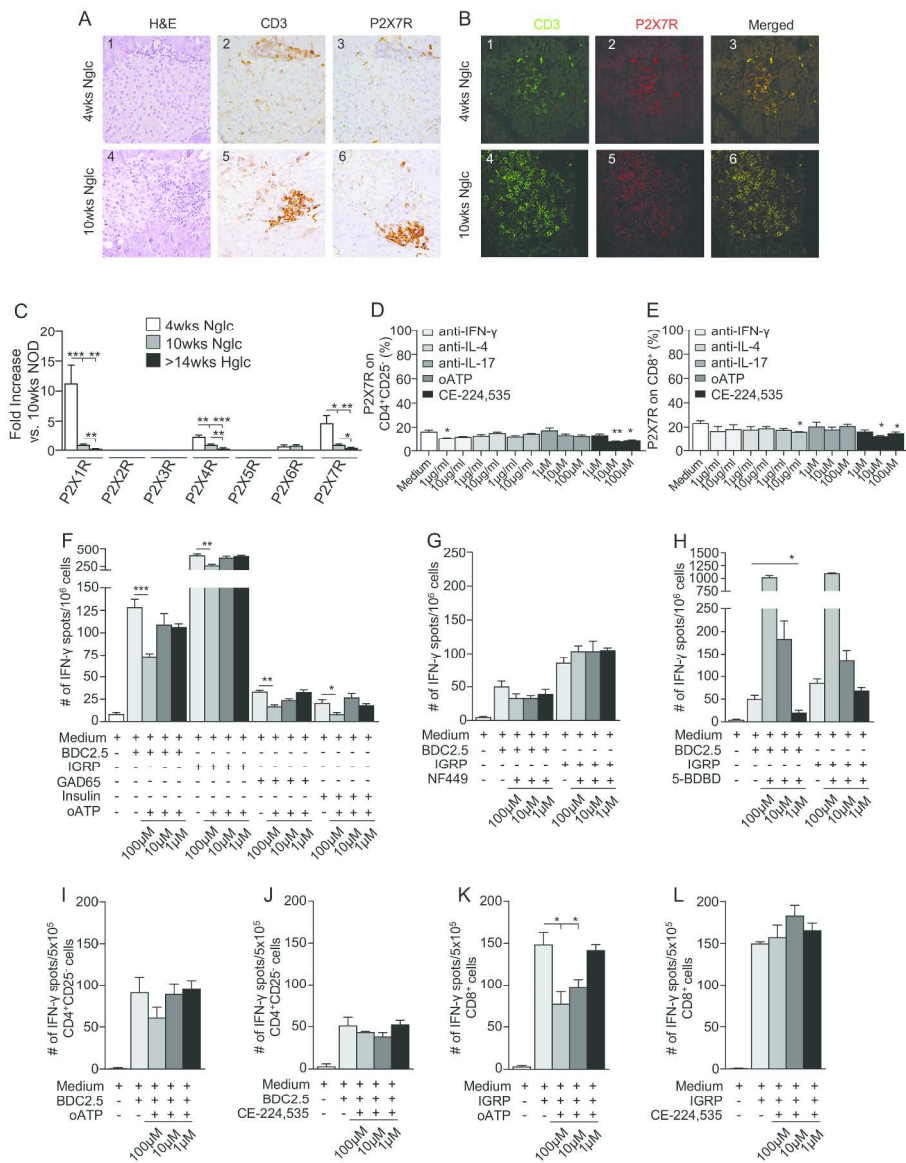


Figure 3

Figure 3

270x361mm (300 x 300 DPI)

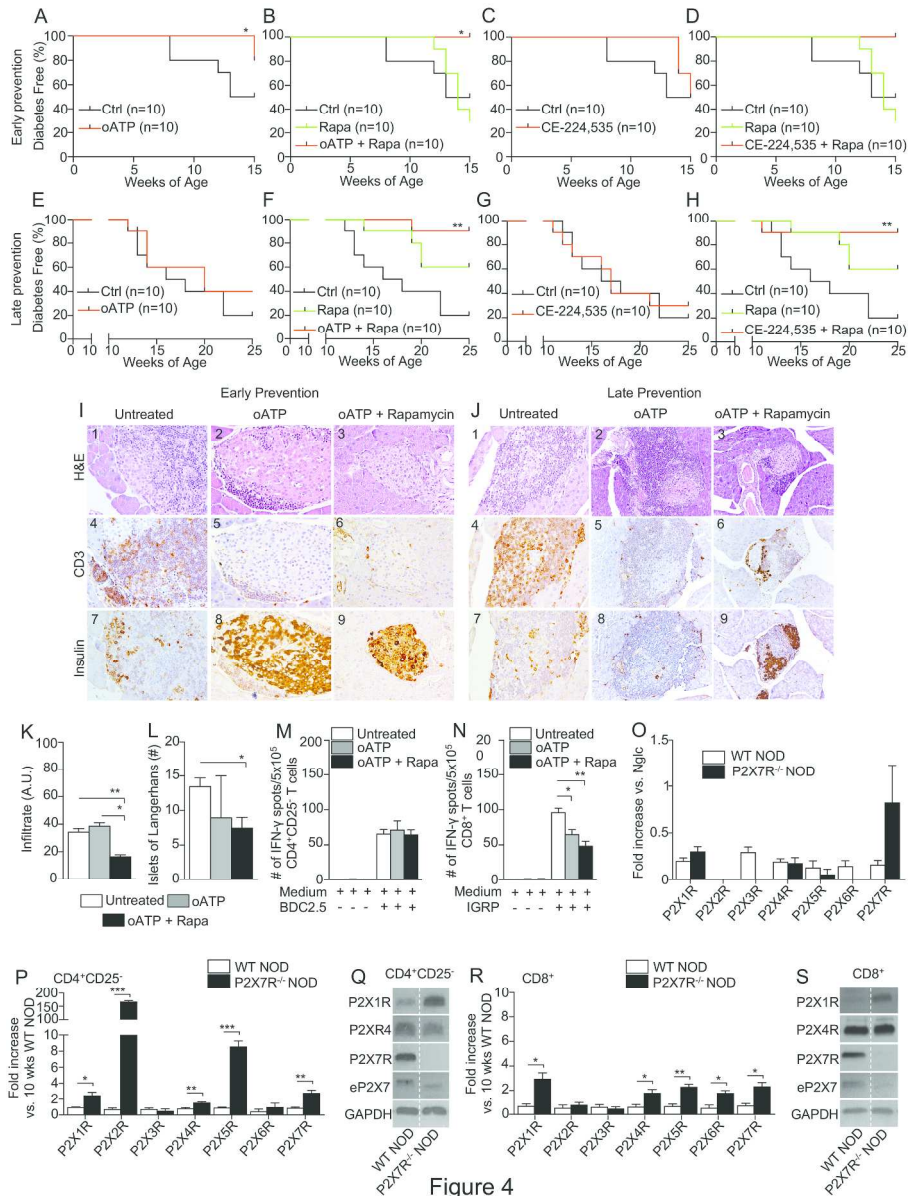


Figure 4

Figure 4

270x361mm (300 x 300 DPI)

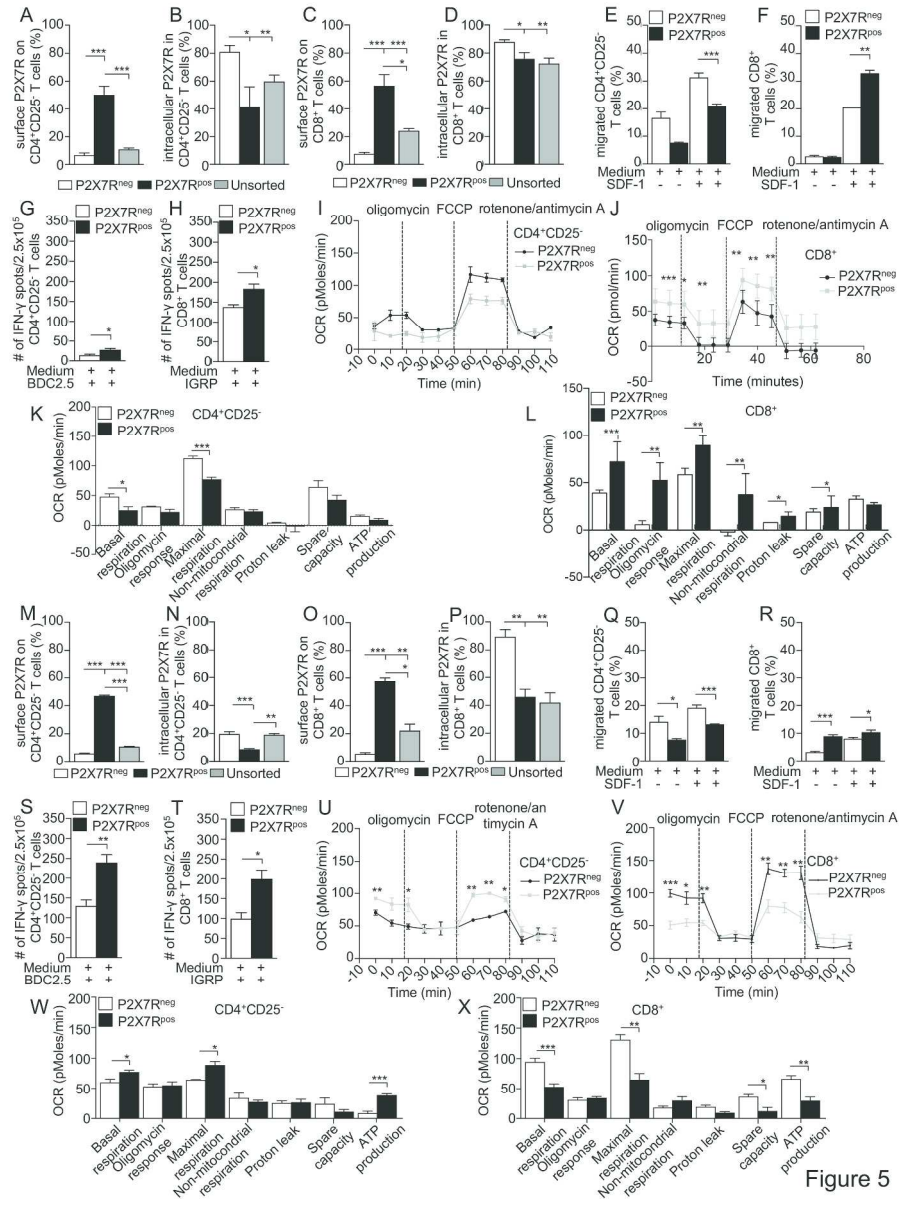


Figure 5

270x361mm (300 x 300 DPI)

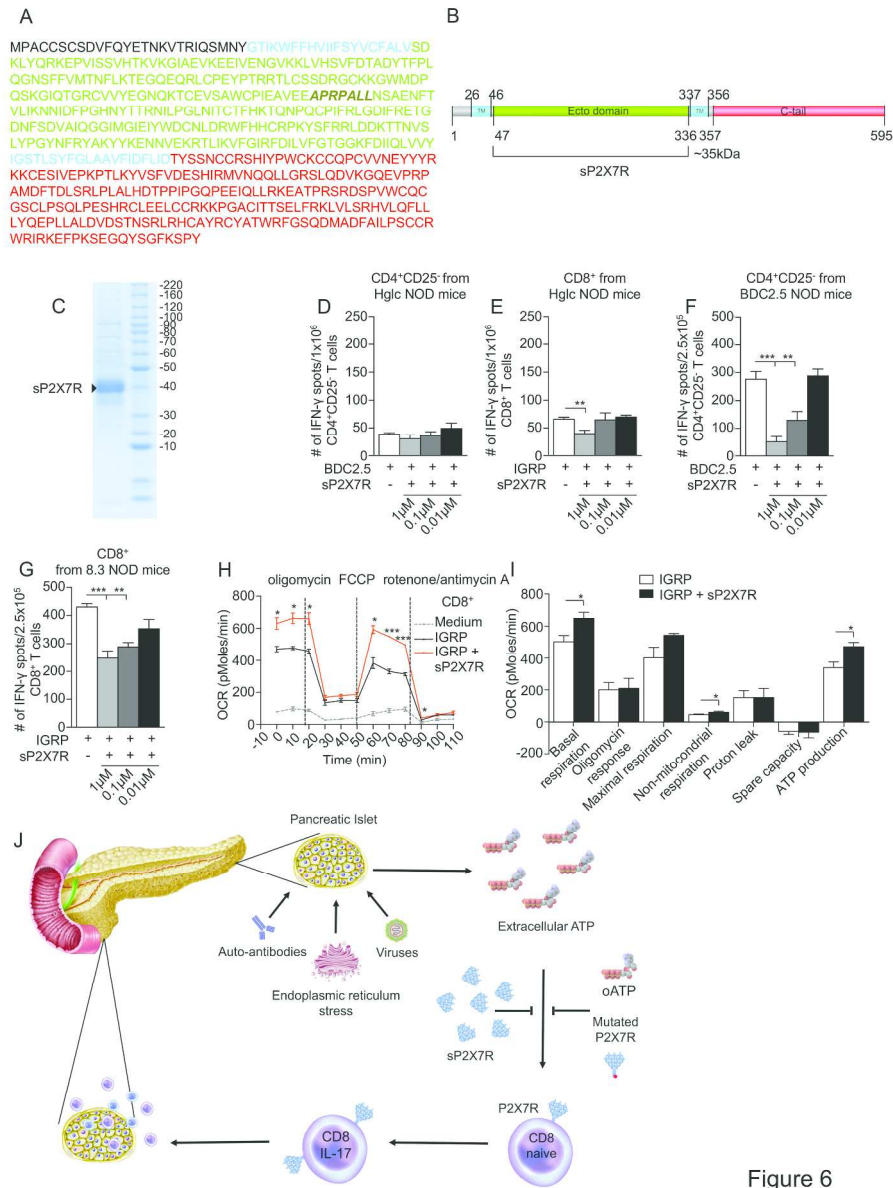


Figure 6

Figure 6

270x361mm (300 x 300 DPI)

**This Supplemental Information file includes:**

**SUPPLEMENTAL DATA:**

**SUPPLEMENTAL FIGURES S1-S5**

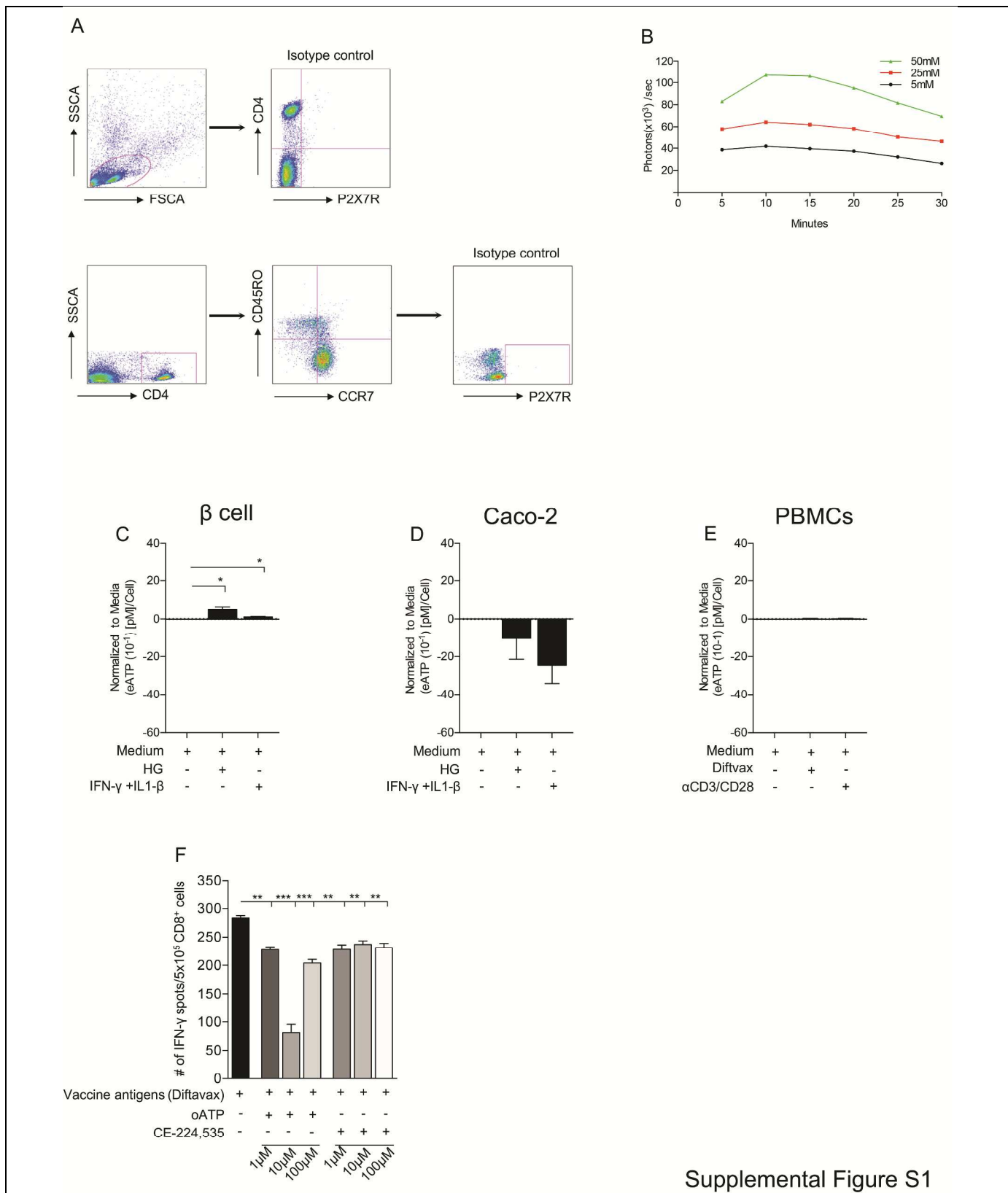
**SUPPLEMENTAL VIDEO S1**

**SUPPLEMENTAL EXPERIMENTAL PROCEDURES**

**SUPPLEMENTAL REFERENCES**

**SUPPLEMENTAL DATA:**

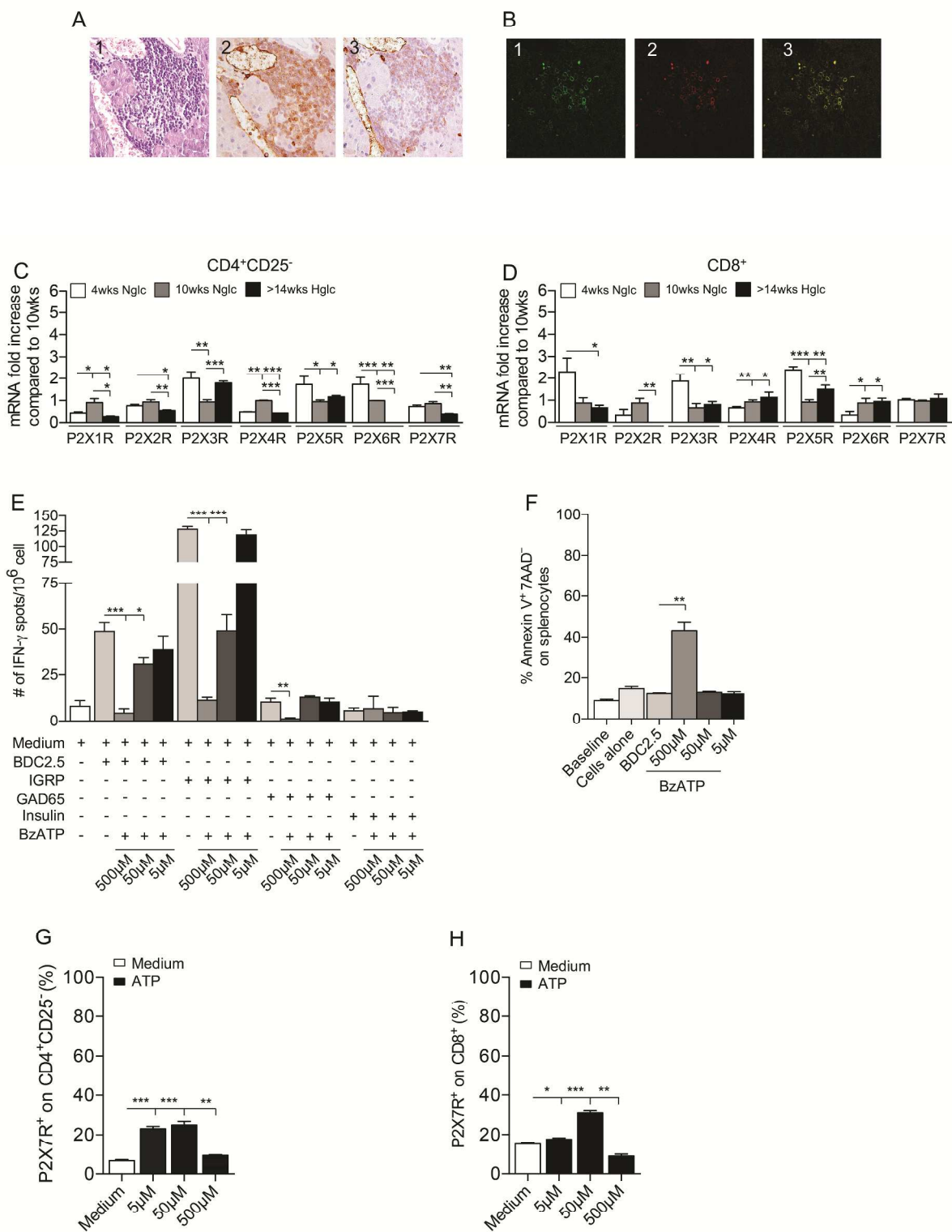
**Supplemental Figures**



Supplemental Figure S1

**Figure S1.** (A) Representative dot plots for P2X7R isotype antibody staining with CD4, CD45RO and CCR7 on human PBMCs are shown, depicting the gating strategy used in Fig. 1D-R. (B) Luminescence signal from pancreas harvested from pmeLUC transgenic mice and cultured in the presence of different glucose concentrations (5, 25 and 50mM) was quantified as photons/second. (C) Bar graph depicting eATP release by the human  $\beta$  cell line Beta-lox5 cultured in high glucose or in the presence of IFN- $\gamma$  (2 ng/ml) and IL-1 $\beta$  (1,000 U/ml) (n=3 samples per group). (D) Bar graph depicting eATP release by the Caco-2 cell line cultured in high glucose or in the presence of IFN- $\gamma$  (2 ng/ml) and IL-1 $\beta$  (1,000 U/ml) (n=3 samples per group). (E) Bar graph depicting eATP release by human PBMCs from T1D patients cultured in the presence of Diftavax or anti-CD3 and CD28 (n=3 samples from each group). (F) Isolated CD8<sup>+</sup> T cells from healthy controls were challenged with antigen vaccines (Diftavax) in the presence or absence of P2X7R antagonists oATP or CE-224,535.

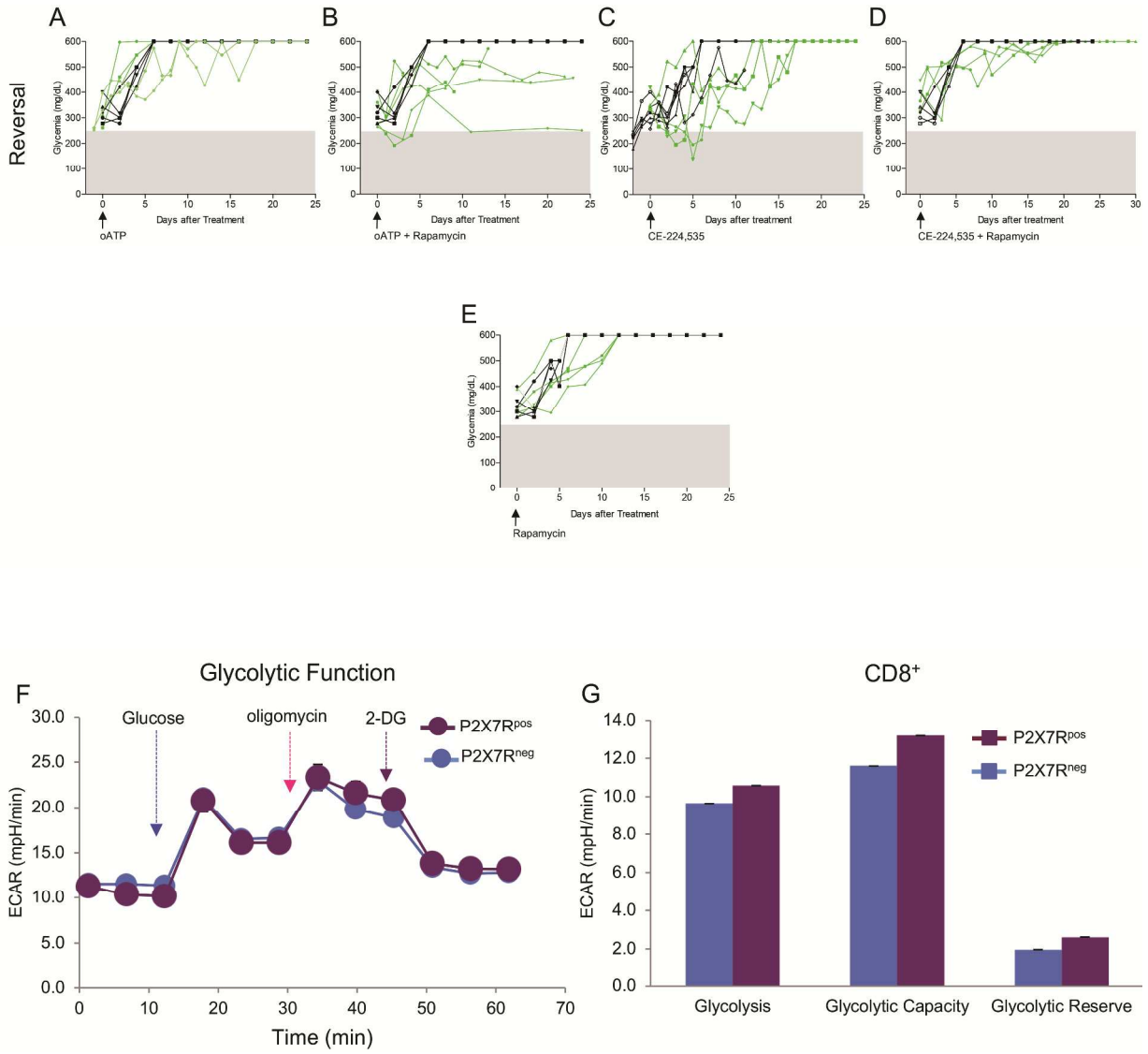
**Abbreviations.** PBMCs (peripheral blood mononuclear cells).



Supplemental Figure S2

**Figure S2. (A, B)** Representative H&E staining and immunohistochemical analysis of CD3 and P2X7R expression on pancreatic islet tissue sections of hyperglycemic NOD mice. **(C, D)** P2XsR mRNA levels were quantified on splenic CD4<sup>+</sup>CD25<sup>-</sup> and CD8<sup>+</sup> isolated T cells from 4- and 10-week-old and hyperglycemic NOD mice, normalized to levels of GAPDH and expressed as fold increase compared to 10-week-old normoglycemic NOD mice. **(E, F)** Splenocytes from hyperglycemic NOD mice were cultured with the CD4/CD8-restricted islet mimotope peptides BDC2.5/IGRP respectively or with GAD65 and insulin, in the presence of different concentrations of BzATP (5, 50, 500 $\mu$ M) in an IFN- $\gamma$  ELISpot assay. High levels of BzATP induced apoptosis of splenocytes as determined by staining for AnnexinV and 7-AAD by flow cytometric analysis. **(G, H)** CD4<sup>+</sup>CD25<sup>-</sup> T cells cultured in the presence of different concentrations of ATP showed a slight but significant upregulation of P2X7R expression on CD4<sup>+</sup>CD25<sup>-</sup> T cells, while in CD8<sup>+</sup> T cells, P2X7R was markedly upregulated, particularly following treatment with 50  $\mu$ M ATP.

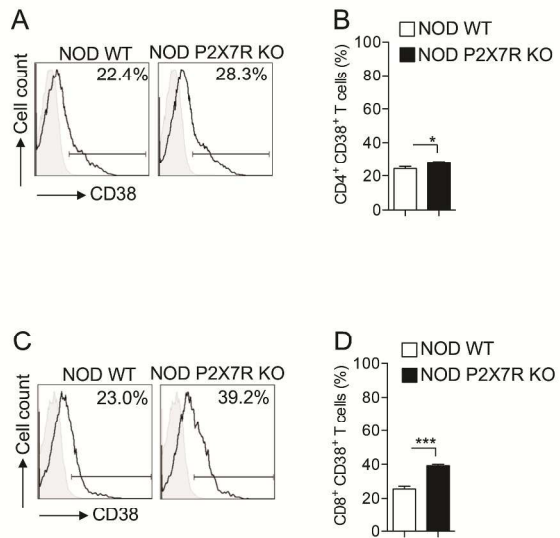
**Abbreviations.** H&E (hematoxylin and eosin); GAPDH (glyceraldehyde-3-phosphate dehydrogenase); BzATP (Benzoyl-ATP); eATP (extracellular ATP); 7-AAD (7-amino-actinomycin D).



Supplemental Figure S3

**Figure S3. (A-E)** The effect of P2X7R blockade was tested in a reversal study using (i) oATP, (ii) CE-224,535, or (iii) a combination of oATP or CE-224,535 with clinical-grade-dose Rapamycin, and Rapamycin alone. **(F-G)** Extracellular acidification rate (ECAR) measurements of CD8<sup>+</sup>P2X7R<sup>pos</sup> and CD8<sup>+</sup>P2X7R<sup>neg</sup> isolated from 10-week-old NOD normoglycemic mice indicate diminished capacity of CD8<sup>+</sup>P2X7R<sup>neg</sup> to mount a glycolytic response.

**Abbreviations.** eATP (extracellular ATP); oATP (oxidized ATP); 2-DG (2-deoxy-D-glucose).



Supplemental Figure S4

**Figure S4. (A-D)** Representative flow cytometric analysis and quantitative bar graphs for CD38<sup>+</sup>CD4<sup>+</sup> T cells (A, B) and CD38<sup>+</sup>CD8<sup>+</sup> T cells (C, D) in splenocytes of P2X7R<sup>-/-</sup> NOD and WT NOD mice.

**Abbreviations.** WT (wild type); NOD (non-obese diabetic).

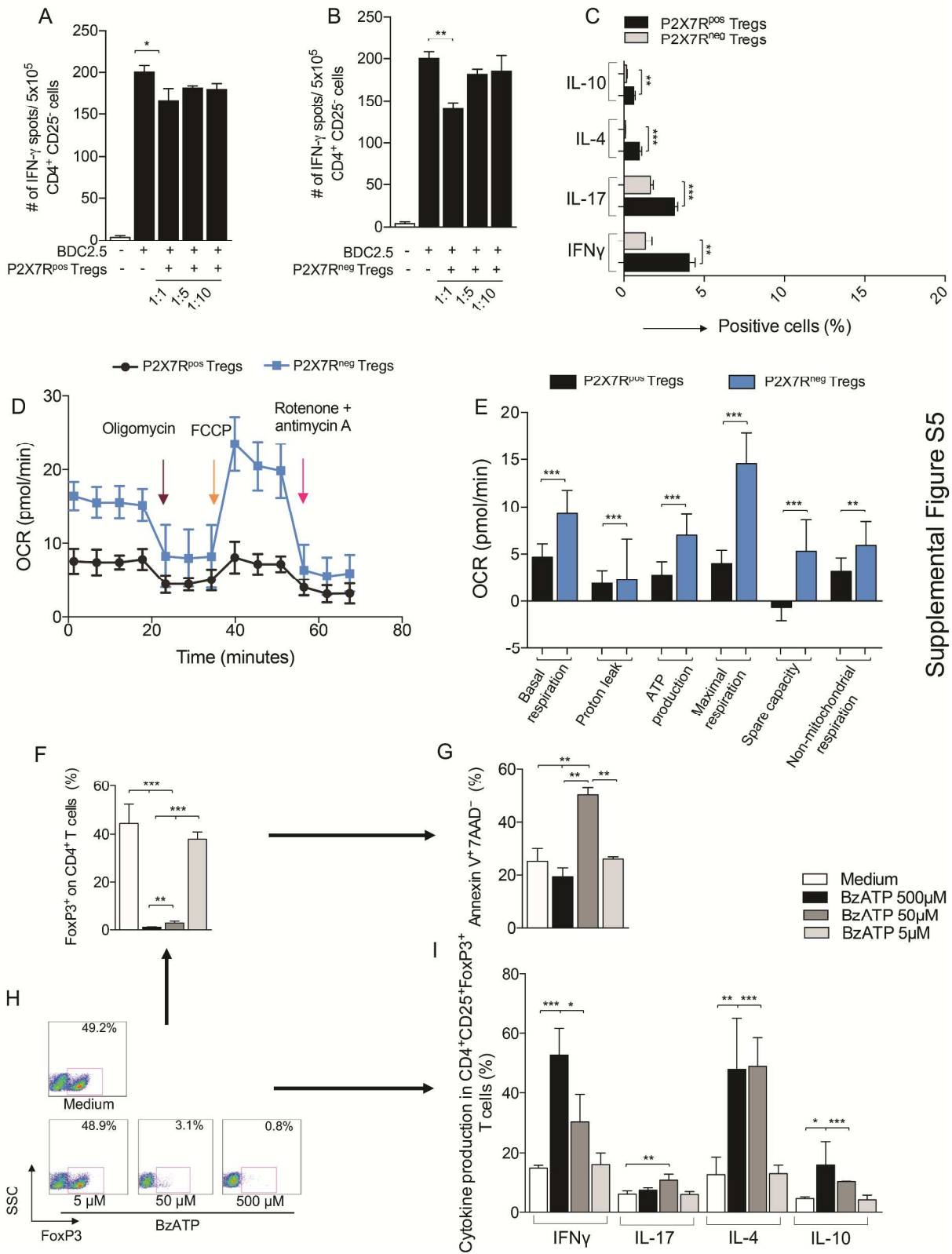


**Figure S5.** (A-B) The immunosuppressive ability of P2X7R<sup>pos</sup> versus P2X7R<sup>neg</sup> Tregs was studied in an ELISpot assay in which CD4<sup>+</sup>CD25<sup>-</sup> TCR tg naïve T cells isolated from NOD BDC2.5 Tg mice were stimulated with BDC2.5 peptides and challenged in a dose-dependent manner (with ratios of 1:1, 1:5, or 1:10 of Tregs to T cells, using either P2X7R<sup>pos</sup> or P2X7R<sup>neg</sup> Tregs). (C) The cytokine profiles of P2X7R<sup>pos</sup> versus P2X7R<sup>neg</sup> Tregs were examined by flow cytometric analysis. (D) Oxygen consumption rate (OCR) measurements using P2X7R<sup>pos</sup> versus P2X7R<sup>neg</sup> Tregs, in which cells were subjected to 1 μM oligomycin, which inhibits ATP synthase and limits mitochondrial OCR. Subsequently, FCCP (cyanide-4-[trifluoromethoxy]phenylhydrazine), which uncouples mitochondrial respiration and maximizes OCR, was added (0.5 μM). (E) Basal respiration and maximal respiration of the P2X7R<sup>pos</sup> versus P2X7R<sup>neg</sup> Treg subsets are shown. (F, H) The effect of BzATP on iTreg generation was determined by assessing Foxp3 expression in an apoptosis assay (G); the cytokine profile of iTregs following *ex vivo* challenge with BzATP was also determined by flow cytometry (I).

**Abbreviations.** WT (wild type); NOD (non-obese diabetic); BzATP, Benzoyl adenosine triphosphate; Tregs, T regulatory cells; iTregs, induced T regulatory cells.



**Video S1.** Video showing the mechanism of action of sP2X7R.

**Abbreviations.** sP2X7R (soluble P2X7R).

## **SUPPLEMENTAL EXPERIMENTAL PROCEDURES**

### ***Murine in vivo imaging***

*In vivo* bioluminescent imaging was performed with an ultra-low noise, high sensitivity cooled CCD camera mounted on a light-tight imaging chamber (IVIS Lumina System, Caliper, PerkinElmer, Waltham, USA). Tracking, monitoring and quantification of signals were controlled by the acquisition and analysis software Living Image (PerkinElmer). NOD and BALB/c mice at 4, 8, 10 and 14 weeks of age were inoculated i.p. with  $2 \times 10^6$  HEK-pmeLUC cells. After cell inoculation, 150 mg/kg (3 mg/mouse) of D-Luciferin (Promega, Madison, WI) was administered i.p. to anesthetized mice with 2% isoflurane 15 minutes before image acquisition. The luminescent signal was captured from ventral view, and Regions Of Interest (ROI) from displayed images were identified and quantified as total photons/second using the Living Image software. This ATP probe or plasma membrane luciferase (pmeLUC) is a chimeric protein previously generated by engineering a firefly luciferase-folate receptor chimeric protein that retains the N-terminal leader sequence and the C-terminal GPI anchor of the folate receptor. Due to the folate receptor leader sequence, pmeLUC is targeted to the plasma membrane and detects ATP in the extracellular milieu close to the cell surface. pmeLUC is sensitive to ATP in the low micromolar to millimolar level, while it is insensitive to all other nucleotides<sup>5</sup>. After 15 minutes following injection, luminescence levels were assessed using an IVIS-Caliper luminometer in the pancreas projection on the abdominal wall.

### ***Murine interventional studies***

Mice were injected i.p with oATP alone, CE-224,535 alone or in combination with Rapamycin (LC Laboratories, Woburn, MA) according to the following therapy protocols: (i) oATP: 8 mg/kg/day i.p. for 4 weeks, (ii) Rapamycin: 0.1 mg/day for 10 days, (iii) oATP+Rapamycin: combination of (i) and (ii), (iv) CE-224,535 0.2mg/kg i.p. for 4 weeks, (v) CE-224,535+Rapamycin: combination of (iv) and (ii).

oATP, Benzoyl-ATP (BzATP; Sigma-Aldrich) and CE-224,535 were used in *in vitro* assays as well.

### ***In vitro* imaging**

For *in vitro* imaging, pancreata from female pmeLUC transgenic mice were collected and incubated for 1 minute at 37°C in Petri dishes containing PBS supplemented with 5 mM glucose. Each pancreas was then transferred to Petri dishes containing 1 ml of PBS supplemented with 5 mM, 25 mM or 50 mM glucose at 37°C. 150 µg/dish of D-luciferin (Promega) were added, and the imaging signal was acquired immediately after using the IVIS system.

### ***Islet culture***

Pancreatic islets were isolated from NOD mice using the collagenase digestion method, as described previously<sup>6</sup>. Islets were cultured at 37 °C in a humidified, 5% CO<sub>2</sub> atmosphere in RPMI 1640 medium (Gibco BRL, Grand Island, NY) supplemented with 10% fetal bovine serum, 2 mM glutamine for 24 or 72h. Murine recombinant IL-1β<sup>7</sup>, IFN-γ<sup>7</sup>, IL-8<sup>8</sup>, and TNF-α were obtained from R&D Systems.

### ***ELISA***

Bioluminescent detection of ATP levels was performed on both human and murine islet culture supernatants, on serum samples from NOD mice at 4 and 10 weeks of age, on serum obtained from hyperglycemic NOD mice, and on supernatant collected after human ELISpot assays using the Enliten ATP assay system (FF2000, Promega) as reported previously<sup>9</sup>. ATP measurements were then performed using a luminometer (Berthold Technologies, Oak Ridge, TN).

### ***Murine antibodies***

The following antibodies were used for flow cytometric analysis in this study: PE-conjugated anti-mouse CD25, -anti-mouse CD44, -anti-mouse P2X7R, peridin-chlorophyll-protein complex-conjugated anti-mouse CD11c, APC-labeled anti-mouse CD4, anti-mouse CD8, anti-mouse CD62L, anti-mouse CD19, and anti-mouse Foxp3 were purchased from BD Biosciences, eBioscience or BioLegend (San Diego,

CA). FITC-conjugated anti-mouse P2X7R was purchased from Alomone Labs. Apoptosis was assessed with the Annexin V Apoptosis Detection Kit I purchased from BD Biosciences, and was analyzed as previously described<sup>10</sup>.

### ***Murine flow cytometric analysis***

To characterize P2X7R expression, murine splenic cells were double-stained with anti-mouse P2X7R and anti-mouse CD4, CD8, CD19 or CD11c. CD4 or CD8 effector T cells were determined by triple staining with CD4 or CD8, anti-mouse CD44 and CD62L, respectively. Regulatory T cells were identified by staining for CD4, anti-mouse CD25, and upon permeabilization using the Fixation/Permeabilization kit (eBioscience) for anti-mouse Foxp3. A FACSCalibur flow cytometer (Becton Dickinson) was used to analyze cells with light scatter properties of lymphocytes. Background staining was determined using nonreactive isotype-matched control mAbs with gates positioned to exclude 99% of non-reactive cells. FlowJo software version 8.7.3 (Treestar, Ashland, OR) was used to analyze the data.

### ***In vitro stimulation of T cells***

To test the effect of T cell stimulation on the expression of P2X7R, CD4<sup>+</sup> CD25<sup>-</sup> T cells were isolated from murine splenic cells using the CD4<sup>+</sup>CD25<sup>+</sup> Regulatory T cell Isolation Kit (Miltenyi Biotec, Auburn, CA). 5x10<sup>5</sup> CD4<sup>+</sup>CD25<sup>-</sup> T cells were cultured in a 96-well plate for 24 hours in the presence of IL-1 $\beta$ , IL-6, TNF- $\alpha$  or MCP-1 at concentrations of 1 or 10 ng/ml (R&D Systems), BzATP and ATP at concentrations of 5, 50 or 500  $\mu$ M (Sigma-Aldrich), anti-mouse IFN- $\gamma$ , anti-mouse IL-4, anti-mouse IL-17 at concentrations of 1 or 10  $\mu$ g/ml (BD Biosciences), oATP (Medestea srl, Turin, Italy) and CE-224,535 (Pfizer, New York, NY) at concentrations of 1, 10 or 100  $\mu$ M. After 24 hours cells were collected and stained with anti-mouse CD4 and anti-mouse P2X7R.

### ***Murine iTreg generation***

CD4<sup>+</sup> Treg differentiation was evaluated by culturing  $2.5 \times 10^5$  naive CD4<sup>+</sup>CD25<sup>-</sup> T cells with plate-bound anti-CD3 and soluble anti-CD28 (both at 1  $\mu\text{g}/\text{ml}$ ) in RPMI1640 media (Lonza, Walkersville, MD) supplemented with 10% FBS (Sigma-Aldrich), 2 mM L-glutamine, 1 mM sodium pyruvate, 0.75 g/L sodium bicarbonate, 100 U/ml penicillin/streptomycin, 0.1 mM non-essential amino acids (all from Lonza) for 2 days with murine TGF- $\beta$ 1 (2 ng/ml), and murine IL-2 (10 ng/ml) at 37°C. After 2 days, 10 ng/ml of murine IL-2 was added to iTreg cultures and incubated an additional 2 days.

### ***Murine apoptosis assay***

Differentiated iTregs cultured in the presence or absence of 5, 50, or 500  $\mu\text{M}$  of Benzoyl-ATP (BzATP; Sigma-Aldrich) were collected and washed twice with cold PBS and then resuspended in 1x Binding Buffer (component no. 51-66121E; BD Biosciences) at a concentration of  $5 \times 10^5$  cells/ml. 100  $\mu\text{l}$  of this solution was transferred into a 5 ml culture tube and was stained with 5  $\mu\text{l}$  of APC Annexin V and 5  $\mu\text{l}$  7-AAD, followed by incubation for 15 min at RT (25°C) in the dark. After incubation, 400  $\mu\text{l}$  of 1x Binding Buffer was added to each tube prior to acquisition on the flow cytometer. We used the following controls as recommended by the manufacturer in order to perform compensation and gating: unstained cells, cells stained with APC Annexin V (no 7-AAD) and cells stained with 7-AAD (no APC Annexin V).

### ***Murine ELISpot assay***

An ELISPOT assay was used to measure the number of IFN- $\gamma$ -producing cells according to the manufacturer's protocol (BD Biosciences) as previously performed by our group <sup>2</sup>. To test the role of eATP/P2X7R-driven immunity on the autoimmune response, we used an islet-peptide based ELISpot assay.  $1 \times 10^6$  splenocytes isolated from hyperglycemic NOD mice were cultured in a microwell plate (BD Biosciences) coated with IFN- $\gamma$  capture antibody (Ab) in the presence of the following islet peptides: BDC2.5 mimotope, IGRP (corresponding to residues 206 to 214 of murine islet-specific

glucose-6-phosphatase catalytic subunit-related protein), GAD (corresponding to residues 206 to 220 of the glutamic acid decarboxylase GAD65) and insulin (Anaspec [Fremont, CA] and Sigma Aldrich respectively) for 24 hours.  $\alpha$ ATP or CE-224,535 at concentrations of 1, 10 or 100  $\mu$ M, BzATP at concentrations of 5, 50 or 500  $\mu$ M, or sP2X7R at concentrations of 0.01, 0.01 or 1  $\mu$ M were also added to the culture. After 24 hours, bound secondary Ab was visualized using HRP-streptavidin and the AEC substrate kit (BD Biosciences). Spots were counted using an Immunospot analyzer (Cellular Technology Ltd., Cleveland, OH) and expressed as the number of cytokine-producing spots per  $1 \times 10^6$  cells. Alternatively,  $CD4^+CD25^-$ ,  $CD8^+$  T cells, and  $CD11c^+$  cells were isolated using the Regulatory T cell Isolation kit, the  $CD8a^+$  T cell Isolation kit or  $CD11c$  MicroBeads (Miltenyi Biotec), respectively.  $5 \times 10^5$   $CD4^+CD25^-$  or  $CD8^+$  T cells were cultured with  $2.5 \times 10^5$   $CD11c^+$  in the presence of BDC2.5 mimotope or IGRP peptide, respectively. After 24h, ELISpot plates were developed as described.  $P2X7R^-$  and  $P2X7R^+$   $CD4^+CD25^-$  or  $CD8^+$  T cells were selected by staining freshly-isolated  $CD4^+CD25^-$  or  $CD8^+$  T cells with PE-conjugated anti-mouse P2X7R antibody, followed by incubation with anti-PE microbeads for selection (Miltenyi Biotec).  $2.5 \times 10^5$   $P2X7R^-$  or  $P2X7R^+$   $CD4^+CD25^-/CD8^+$  T cells were co-cultured with  $1.25 \times 10^5$   $CD11c^+$  cells and BDC2.5 or IGRP, respectively. After 24h, ELISpot plates were developed, or cells were collected and P2X7R expression was assessed by flow cytometry, as described.

### ***Histopathology and immunohistochemistry***

Immunohistochemistry was performed with 5  $\mu$ m-thick formalin-fixed, paraffin-embedded pancreatic tissue sections as described previously <sup>6</sup>. Photomicrographs (400x or 200x) were taken using an Olympus BX41 microscope (Center Valley, PA). The following primary antibodies were used: anti-CD3 (Cell Marque, Rocklin, CA), anti-Foxp3 (eBioscience), anti-insulin (Dako North America, Carpinteria, CA) and anti-P2X7R (Alomone Labs). Graft histology was evaluated by an expert pathologist and was quantified as follows: (i) *Insulin staining*: 0: no insulin staining, 1: presence of scattered insulin-positive

cells, 2: presence of insulin-positive cell aggregates, 3: presence of preserved insulin-positive islets; (ii) *Islet cell infiltrate*: 0: no cell infiltrate, 1: presence of cell infiltrate around graft islets, 2: presence of cell infiltrate inside graft islets, 3: presence of cell infiltrate throughout the graft area without preserved islet structure.

### ***Confocal microscopy***

All immunofluorescence samples were observed using a confocal system (LSM 510 Meta scan head integrated with the Axiovert 200 M inverted microscope; Carl Zeiss, Jena, Germany) with an 63x oil objective. The images were acquired in multi track mode, using consecutive and independent optical pathways<sup>11</sup>. The number of CD3<sup>+</sup>/P2X7R<sup>+</sup> cells was assessed by counting the number of orange-stained elements (the result of green and red signal super-imposition) in 10 histological fields at x63, respectively.

### ***Quantitative real-time PCR***

Total RNA was extracted from CD4<sup>+</sup>CD25<sup>-</sup>, CD8<sup>+</sup> isolated T cells or from whole pancreas after homogenization. RNA was purified using an RNeasy kit (Qiagen, Valencia, CA) and was reverse-transcribed into cDNA using Superscript III (Invitrogen, Carlsbad, CA). Transcripts were amplified using a 7300 Real-Time PCR System and primers from Applied Biosystems (Foster City, CA), normalized to copies of GAPDH and quantified by comparison to 10-week-old NOD mice. NOD-P2X7R knock out RNA was isolated from pancreatic tissue sections and reverse-transcribed into cDNA as described. Amplified transcripts were normalized to GAPDH and number of islets, and quantified by comparison to 10-week-old NOD.

### ***Western blot***

Total protein of CD4<sup>+</sup>CD25<sup>-</sup> T cells samples were extracted using Laemmli buffer (Tris-HCl 62.5 mmol/l, pH 6.8, 20% glycerol, 2% SDS, 5% β-mercaptoethanol), and their concentrations were

measured. 35  $\mu\text{g}$  of total protein was electrophoresed on 7% SDS-PAGE gels and blotted onto nitrocellulose (Schleicher & Schuell, Dassel, Germany). Blots were then stained with Ponceau S. Membranes were blocked for 1 h in TBS (Tris [10 mmol/l], NaCl [150mmol/l]), 0.1% Tween-20, 5% non-fat dry milk, pH 7.4 at 25°C, and then incubated for 12 h with rabbit anti-P2X7R (Alomone Labs #APR-004), rabbit anti-mouse P2X7R (Alomone Labs #APR-008), rabbit anti-mouse P2X4 (Alomone Labs #APR-002), rabbit anti-mouse P2X1 (Alomone Labs #APR-001) or rabbit anti-mouse GAPDH (Cell Signaling, Danvers, MA) diluted in TBS–5% milk at 4°C. Membranes were washed three times with TBS–0.1% Tween-20, then incubated with a peroxidase-labeled anti-rabbit IgG antibody (ECL™, #NA934) diluted 1:500 in TBS–5% milk, and finally washed with TBS–0.1% Tween-20. The resulting bands were visualized using enhanced chemiluminescence (SuperSignal; Pierce, Rockford, IL, USA). Finally, for the quantification of western blot bands, images of nitrocellulose membrane filters were analyzed by ImageJ software to quantify size and strength of protein bands.

### ***Migration assays***

Transwell migration assays were performed on isolated P2X7R<sup>-</sup> or P2X7R<sup>+</sup> CD4<sup>+</sup>CD25<sup>-</sup> or CD8<sup>+</sup> T cells in the presence of 0 to 50 ng/ml SDF-1 (R&D Systems). In brief, cells were suspended in 0.5% BSA Phenol Red-Free RPMI and plated in the upper chambers of an HTS-Transwell-96-well permeable support plate (Corning, Acton, MA). After overnight incubation, migrated cells were counted using BD TruCount (BD Biosciences) by flow cytometry.

### ***Metabolic assays***

We measured the bioenergetic function (oxygen consumption rate or OCR) of sorted P2X7R<sup>-</sup> or P2X7R<sup>+</sup> CD4<sup>+</sup>CD25<sup>-</sup> or CD8<sup>+</sup> T cells using a XF24 and XF96 Extracellular Flux Analyzer (Seahorse Bioscience, North Billerica, MA). P2X7R<sup>neg</sup> or P2X7R<sup>pos</sup> CD4<sup>+</sup>CD25<sup>-</sup> or P2X7R<sup>neg</sup> or P2X7R<sup>pos</sup> CD4<sup>+</sup>CD25<sup>+</sup> or CD8<sup>+</sup> T cells were resuspended in XF media (RPMI containing 25 mM glucose, 2 mM L-glutamine, and

1 mM sodium pyruvate adjusted to pH 7.4), and  $4 \times 10^5$  cells per well were plated in XF24 and XF96 plates previously coated using CellTak (BD Biosciences) in order to enhance cell adherence. OCR measurements were assessed under basal conditions (3 measurements were taken) and in response to 2  $\mu$ M oligomycin, 1.5  $\mu$ M fluoro-carbonyl cyanide phenylhydrazone (FCCP), and 1  $\mu$ M rotenone + 1  $\mu$ M antimycin A with the XF24 or XF96 analyzer (Seahorse Bioscience), at a rate of 3 measurements after injection of each compound. In another assay, we assessed glycolytic function (extracellular acidification rate, or ECAR) of sorted P2X7R<sup>-</sup> or P2X7R<sup>+</sup> CD8<sup>+</sup> T cells. ECAR measurements were taken when cells were exposed to 10 mM glucose, 2  $\mu$ M oligomycin and 50 mM of 2-Deoxy-D-glucose. 3 baseline measurements of ECAR were taken, and 3 measurements were taken after injection of each of the 3 compounds (glucose, oligomycin and 2-Deoxy-D-glucose).

#### ***Construction of the soluble P2X7R recombinant protein***

A construct encoding the fragment of human P2X7R containing amino acids 56-328 was amplified by PCR from P2X7R cDNA (NP\_002553.3) using primers with the following sequences: 5'-CTGTATTTTCAGGGCGCCATGGATCCTGTCATCAGTTCTGTGCAC-3' and 5'-CTCTAGTACTTCTCGACAAGCTTCATCAAAATTTTCTCCGGTGCCAAAAC-3'. The amplified product was cloned into the pFHMSp-LIC-N donor plasmid, which is a derivative of the pFastBac HT A vector (Invitrogen) for directing secreted protein expression in insect cells via the Baculovirus Expression System. The pFHMSp-LIC-N vector has the Honeybee melittin signal sequence upstream of the poly-His tag and a SacB gene stuffer sequence subcloned between NcoI/HindIII restriction sites in the multiple cloning site sequence. The modified vector is supplied with a 26-amino acid N-terminal fusion tag containing 6X His followed by a TEV cleavage site, which are added in frame with the inserted coding sequence. The P2X7R 56-328 fragment was inserted into the cloning region of the NcoI/HindIII linearized pFHMSp-LIC-N using In-fusion (BD Biosciences) enzyme-mediated

recombination of complimentary DNA sequences that were inserted at the ends of the insert by engineered primer design and are present in the vector.

### ***Generation of recombinant Bacmid DNA and baculovirus***

DH10Bac *E.coli* cells (Invitrogen) were transformed with the recombinant donor vector pFHMSD-P2X7R to generate recombinant viral DNA. Sf9 insect cells (Invitrogen) were transfected with the Bacmid DNA using Cellfectin reagent (Invitrogen), and recombinant baculovirus particles were recovered in the supernatant. The recombinant virus was sequentially amplified from P1 to P3 viral stocks before expression.

### ***Expression and purification of recombinant soluble P2X7R in insect cells***

Sf9 insect cells were grown in HyQ<sup>®</sup> SFX Insect Serum Free Medium (GE Healthcare Life Sciences) infected with P3 viral stock, and cultured at 27°C on a shaker at 100 RPM. At day 4 post-infection, cell culture medium was collected, centrifuged at 14,000 g for 15 minutes, and the cell pellet discarded. The collected medium was neutralized adding 10x binding buffer (50 mM HEPES pH 7.5, 2400 mM NaCl, 50 mM imidazole) and rocked with pre-equilibrated NiNTA beads. The resin was washed twice with two washing buffers (50 mM HEPES pH 7.5, 500 mM NaCl, 10 mM imidazole; 50 mM HEPES pH 7.5, 500 mM NaCl, 40 mM imidazole). The bound protein was eluted with elution buffer (50 mM HEPES pH 7.5, 500 mM NaCl, 250 mM imidazole) and loaded onto a Superdex 200 10/300GL gel filtration column (GE Healthcare, Boston, MA) equilibrated with 20 mM HEPES pH 7.5, 150 mM NaCl. The relevant fractions containing protein were pooled and concentrated by ultrafiltration using an Amicon Ultra-15 10 kD MWCO filter unit (Millipore, Billerica, MA) to 2.4 mg/ml, with an overall yield of 2 mg/L.

### ***Statistical analysis***

Data are expressed as mean±standard error of mean. Kaplan-Meier analysis was used for analysis of survival. When 2 groups were compared, a two-sided unpaired Student t-test (for parametric data) or a

Mann-Whitney test (for non-parametric data) was used, according to distribution. A *P* value of less than 0.05 (by two-tailed testing) was considered to be an indicator of statistical significance. Data and graphs were generated using GraphPad Prism version 5.0 (GraphPad Software, San Diego, CA).

## **SUPPLEMENTAL REFERENCES**

1. Mueller PW, Rogus JJ, Cleary PA, et al. Genetics of Kidneys in Diabetes (GoKinD) study: a genetics collection available for identifying genetic susceptibility factors for diabetic nephropathy in type 1 diabetes. *J Am Soc Nephrol* 2006;17:1782-90.
2. Petrelli A, Carvello M, Vergani A, et al. IL-21 is an antitolerogenic cytokine of the late-phase alloimmune response. *Diabetes* 2011;60:3223-34.
3. Ardestani A, Paroni F, Azizi Z, et al. MST1 is a key regulator of beta cell apoptosis and dysfunction in diabetes. *Nat Med* 2014;20:385-97.
4. Lightfoot YL, Chen J, Mathews CE. Role of the mitochondria in immune-mediated apoptotic death of the human pancreatic beta cell line betaLox5. *PLoS One* 2011;6:e20617.
5. Pellegatti P, Falzoni S, Pinton P, Rizzuto R, Di Virgilio F. A novel recombinant plasma membrane-targeted luciferase reveals a new pathway for ATP secretion. *Mol Biol Cell* 2005;16:3659-65.
6. Vergani A, D'Addio F, Jurewicz M, et al. A novel clinically relevant strategy to abrogate autoimmunity and regulate alloimmunity in NOD mice. *Diabetes* 2010;59:2253-64.
7. Lv N, Kim EK, Song MY, et al. JANEX-1, a JAK3 inhibitor, protects pancreatic islets from cytokine toxicity through downregulation of NF-kappaB activation and the JAK/STAT pathway. *Exp Cell Res* 2009;315:2064-71.

8. Lin CH, Nai PL, Bien MY, Yu CC, Chen BC. Thrombin-induced CCAAT/enhancer-binding protein beta activation and IL-8/CXCL8 expression via MEKK1, ERK, and p90 ribosomal S6 kinase 1 in lung epithelial cells. *J Immunol* 2014;192:338-48.
9. Vergani A, Fotino C, D'Addio F, et al. Effect of the purinergic inhibitor oxidized ATP in a model of islet allograft rejection. *Diabetes* 2013;62:1665-75.
10. Carvello M, Petrelli A, Vergani A, et al. Inotuzumab ozogamicin murine analog-mediated B-cell depletion reduces anti-islet allo- and autoimmune responses. *Diabetes* 2012;61:155-65.
11. Corradi D, Callegari S, Benussi S, et al. Regional left atrial interstitial remodeling in patients with chronic atrial fibrillation undergoing mitral-valve surgery. *Virchows Arch* 2004;445:498-505.